Development of a test stand for the evaluation of row crop planter automatic downforce systems and the evaluation of a row crop planter electronic drive singulation seed meter.

by

Ryan Scott Strasser

B.S., Kansas State University, 2017

A THESIS

submitted in partial fulfillment of the requirements for the degree

MASTER OF SCIENCE

Department of Biological and Agricultural Engineering
College of Engineering

KANSAS STATE UNIVERSITY
Manhattan, Kansas

2017

Approved by:

Major Professor
Dr. Ajay Sharda

Copyright

Abstract

In recent years, the technology employed on precision row-crop planters has rapidly advanced. These new technologies include automatic downforce control systems and electronic drive singulation seed meters. These new technologies offer producers higher productivity through high speed planting and increased yield potentials through accurate seed spacing and placement. To begin to understand the benefits and performance of these new technologies, research must be conducted that specifically targets these new systems. With this research, producers would be able to better select equipment for their operation and have a deeper understanding of proper system operation and settings.

A test stand, of a scissor-lift type design, was developed to evaluate row crop planter automatic downforce systems. Evaluation of a planter's automatic downforce system is important for understanding the planter's capability of maintaining target seeding depth throughout varying field conditions. The test stand consists of a horizontal platform that can raise and lower to simulate terrain changes as well as a mechanism to load the planter row unit's opening discs to simulate varying soil texture. The vertical height of the test stand and the disc load can be varied in real-time based on utilizing real-world scenarios under simulated conditions to evaluate downforce system response. The stand incorporated several sensors to obtain the overall applied downforce, applied disc load, applied gauge wheel load, and hydraulic pressure.

The test stand's capabilities were evaluated and found to be satisfactory for planter downforce system testing. The test stand was then used to evaluate a commercial automatic downforce system when operating under simulated field conditions. Field data was used to create simulations representing soil type changes, planter operating speed changes, and extreme

conditions such as a hard, packed clay or rocky soil type. It was found that the evaluated downforce system was able to maintain target gauge wheel load to within ±223 N for at least 94% of the time during all simulations. This would suggest that the planter would be able to maintain target seeding depth for at least 94% of field operations.

Another key aspect for precision agricultural planters is to achieve accurate seed spacing at varying speeds. An electronic drive singulation seed metering system was evaluated to gather the meter's effectiveness for high speed planting during straight and contour farming mode using simulated field conditions. The simulated conditions were used to gather the meter's response when encountering high planting speeds, accelerations, decelerations, point-rows, and contours. These meters were found to be highly accurate, with less than 1.5% error in target seed meter speed during all simulated conditions. The meters were also found to have a response time that was always 0.34 seconds or less for all simulated conditions.

Table of Contents

List of Figures

List of Tables

Acknowledgements

Special thanks is extended to the Kansas State University Biological and Agricultural

Engineering Department for the testing space, supportive funding, data acquisition hardware and

software. Special thanks is also extended for guidance and support to conduct the research from

Dr. Daniel Flippo, Dr. Ajay Sharda and Jon Zeller. Similarly, Horsch's support during this

research was greatly appreciated when correctly configuring the planter systems for the

respective tests.

Chapter 1 - Introduction

With recent advancements in planting technology, such as automatic downforce control and electronic drive singulation seed metering systems, producers have the ability to apply precision agricultural practices easier than ever before. By applying advanced precision agricultural practices, producers can reduce planting expenses by conservation of seed and field resources by placing the correct amount of seeds required in their proper place. To accomplish this, many new technologies have emerged in the row crop planter marketplace. Singulation seed metering systems can be ground driven, hydraulically driven, and electronically driven. A planter's downforce can be controlled through springs, pneumatics, or hydraulics.

A typical electronic drive singulation seed metering system consists of individually driven row units that can each be operated at a different speed. The use of electronic drive singulation seed meters allows for turn compensation, point-row engagement and disengagement, and acceleration and deceleration compensation. By compensating for these occurrences, seeds are always placed at their proper spacing, even while the planter is experiencing a contour, and over-seeding and under-seeding is eliminated. This allows for each plant to always receive the same allotment of space, thereby presenting each seed with nearly the same growing conditions.

By utilizing individual row point-row control, an electronic drive singulation seed metering system can eliminate overlap caused by section controlled planters which engage and disengage several rows at one time. Section control leads to planter rows overlapping previously planted areas which doubles the rate of seeds planted in the overlapped area leading to unequal growing conditions and wasted seeds.

A typical row crop planter automatic downforce control system consists of a means to control the downward force applied to a row unit, or section of row units, based on a row-unit mounted load sensor so that a controller can compensate for varying field conditions and reduce or eliminate the over or under application of downforce. If downforce is under applied the planter row units may not reach the desired seeding depth thereby affecting plant performance and possibly causing a reduction in yield. If downforce is over applied, seeding depth can be increased beyond the target seeding depth and compaction can be created around the planted seeds. This can also cause a possible reducing in plant performance and yield.

Motivation

The advancement of production precision planting systems, specifically electronic drive singulation seed meters and automatic downforce systems, has happened within the last 10 to 15 years with limited research evaluating their performance and potential. By evaluating the performance of a typical electronic drive singulation seed meter, the performance of this system can be gathered and related to previous planting technologies and used to determine their cost effectiveness. Once the performance of these electronic meters is determined, it can be used when evaluating the planter row unit's overall seed singulation, delivery, and seed placement system to attribute a certain amount of overall system error to the electronic metering drive component itself. Then other components of the seed singulation, delivery, and seed placement system, such as the seed delivery tube or brush belt, furrow opening and closing apparatuses, or firming wheels, can be evaluated for their individual error. This would allow certain areas of the singulation, delivery, and seed placement system to be targeted for improvements to further reduce overall system error.

With the evaluation of an automatic downforce control system, the ability of the system to maintain proper downforce and seeding depth can be determined. This performance can then be compared to other downforce technologies such as pneumatic systems, spring systems, or hydraulic systems. By comparing technologies, the advantages and disadvantages of each system can be determined and compared. This information would be helpful for producers trying to decide which system is adequate for their operation.

To evaluate downforce systems, there has previously been no methods for static lab evaluation. By using a lab-based evaluation environment, the varying effects seen in-field by row crop planters can be controlled and replicated to gain an overall understanding of the differences and performances of each particular downforce system.

Objectives

With the previous ideas in mind, the following objectives were established for the research included in this paper:

1. Develop a downforce evaluation test stand for static lab use to evaluate the performance of various commercially available downforce systems.

2. Evaluate the performance and capabilities of the designed test stand through lab simulations.

3. Use the downforce test stand to do preliminary evaluations of a commercially available automatic hydraulically actuated downforce system.

4. Determine the performance of electronic drive singulation seed metering systems during simulated field conditions of contour, point-row, and acceleration and deceleration scenarios.

Chapter 2 - Development of an Automatic Planter Downforce Evaluation Test Stand to Quantify System Response and Accuracy

In recent years, great improvements have been made in row crop planter design. Many of these improvements were focused around seed metering and delivery to the in-soil furrow and the ability to maintain proper seed spacing. Accurate seed placement is critical for uniform spacing, achieving target population, and providing optimum yield potential (Nielsen, 2005), (Zhao, Chen, 2015). In addition to spacing seed, uniform depth is a vital parameter for achieving uniform emergence (Nielsen, 2004). With increases in seed metering accuracy, other areas of the planter must be addressed to further improve seed placement and take full advantage of these highly accurate seed meters. Recently, researchers have turned their focus to the soil engaging components that open a furrow, place a seed, and then close the furrow.

By properly placing the seed in the available soil moisture zone, seed germination and emergence can be maximized to maximize yield potential (Sharda et al., 2017). Also, during planting in a field of one soil type, the ERI, or emergence rate index, of corn is affected by varying levels of downforce (Hanna, Steward, Aldinger, 2010). Studies have shown that the level of downforce applied can significantly affect seeding depth. The research presented the evidence that if downforce was over-applied, the seeding depth was increased, whereas if the downforce was under-applied, the seeding depth was decreased (Hanna, Steward, Aldinger, 2010).

In recent years, new methods of controlling and applying planter row unit downforce have emerged. The traditional-style spring downforce systems have been nearly replaced by either pneumatic, hydraulic, or electronic downforce mechanisms. The spring systems were replaced

due to the effects of a spring increasing or decreasing its applied load as it is extended or retracted when the planter row unit follows the contours of the land (Morrison, 1988). The changes in spring force as the row unit followed the contours of the land resulted in adverse effects on seeding depth uniformity (Morrison, 1988). The new systems, hydraulic, pneumatic, and electronic, allow the operator to easily adjust the applied downforce to all row units from the tractor operator seat. Many systems utilizing these new methods for downforce application control the desired downforce across the entire planter and cannot provide row-by-row or section based downforce control. Some of these systems incorporate load sensors that utilize row unit gauge wheel loading to adjust downforce through the field, such as Precision Planting's Delta Force system (Precision Planting, Tremont, Illinois). Another method for maintaining optimal seeding depth has been developed by E.T. Weatherly (1997) that utilizes a forward-mounted moisture sensor that is used to control the actual gauge wheel height to vary seeding depth based upon real-time moisture measurements.

On a typical planter row unit, there are three main soil-engaging components; the closing wheels, gauge wheels, and opening discs. The gauge wheels ride across the field surface to prevent the opening discs from penetrating deeper than the seed depth setting. To keep the gauge wheel in contact with the soil, vertical downward force must be applied to the row unit until the proper seed depth is reached, the gauge wheels have reached a target load, and the press wheels are in full contact with the ground (Morrison, 1988). At a certain depth setting, the opening discs will only require a specific amount of downforce to reach the set seeding depth (Morrison et al., 1996). The required disc load changes with soil type, texture, moisture, and terrain, so overall applied downforce must be adjusted (Sharda et al., 2017). By adjusting the applied downforce, a target gauge wheel load can be maintained that prevents overloading or under loading of the

gauge wheels that could cause compaction or improper seeding depths (Morrison et al., 1996). Because soil texture and moisture throughout a field affect required disc loading, trends in soil moisture and texture can be mapped using soil EC measurements (Grisso et al., 2009), and used to infer changes in disc loading that will occur.

Currently, no method has been developed to statistically evaluate the automatic downforce control systems on row crop planters. With limited tests to evaluate planter downforce systems, additional studies are needed to better understand how automatic downforce control systems respond as well as the effects of changes in opening disc loading and their effects on gauge wheel loading. To evaluate the response and accuracy of these automatic hydraulic downforce systems and better understand the relationship between the opening disc loading and gauge wheel loading, the following objectives were established:

Objectives

• Develop a test stand to statically evaluate planter hydraulic downforce systems within a lab-based environment

• Evaluate test stand operational performance and capabilities

• Quantify hydraulic planter downforce control system response to simulated soil and terrain changes

Methodology

Downforce Test Stand Capabilities

To analyze the accuracy and response of hydraulic downforce control systems under real-world field scenarios, a downforce test stand was designed, constructed, and evaluated. The test stand was designed to support the load of a Horsch Maestro (Horsch Maschinen GmbH, Schwandorf, Germany) seeding row unit and withstand the additional load added through the hydraulic system during automatic downforce control system (Horsch Maschinen GmbH, Schwandorf, Germany) operation. The row unit operation was controlled using a Horsch field computer connected to the planter electric control unit, hence forth referred to as an ECU, (Horsch Maschinen GmbH, Schwandorf, Germany) through the planter's ISOBUS.

The test stand consisted of a horizontal, suspended platform, of a scissor-lift type design to support and engage with the row unit, Figure 2-1. The test stand has the capability to separately load the planter row unit's gauge wheels and opening discs as well as the ability to change the row unit's operating height using pneumatic controls. The row unit's gauge wheel placement and dimensions, row unit weight, and magnitude of load that the hydraulic downforce system applied was derived from the manufacturer's product literature, drawings and personal meetings. Based on row unit weight and hydraulic downforce system capability, the test stand was designed for a maximum load capacity of 4454 N. Additionally, the test stand incorporates a vertical travel mechanism to raise and lower the height of the platform and a disc loading mechanism to simulate soil resistance so that the planter's downforce system feedback and response can be gathered.

8
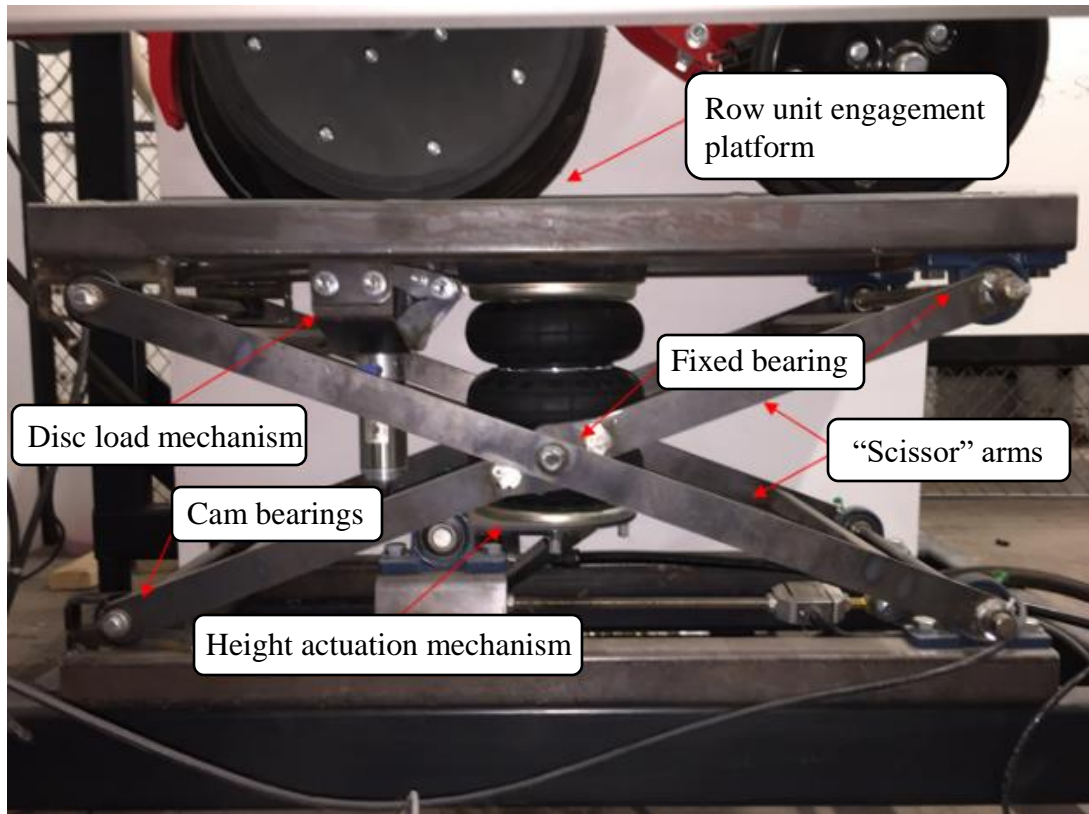
Figure 2-1 Automatic downforce evaluation stand with a row unit mounted above

Design of Test Stand Mechanics

The test stand was designed by considering the load applied by the planter row unit during operation, the planter row unit design, the load bearing (or soil engaging) component placement, and the desired stand mechanics that would generate disc loading and entire row unit vertical travel representative of real-world scenarios of a planter travelling through varying terrain. Also, the platform where the row unit engages with the test stand was required to remain horizontal throughout the stand's vertical travel motions. The horizontal platform simulates the row unit's interaction with the soil surface in a field. In order to keep the platform horizontal, a scissor-lift type mechanism was chosen for the basic test stand design. The size of the platform was chosen

by evaluating the dimensions and placement of opening discs and gauge wheels on the row unit.

The test stand was constructed out of steel square tubing, sheet steel, flange bearings, shafts,

fasteners, and pneumatic components. The scissor-lift type mechanism incorporated fixed

bearings on one end of the scissor arms and cam-follower bearings on the opposite that follow

fabricated channels Figure 2-1. The length of the fabricated cam follower channel set the

maximum and minimum height of the test platform to prevent over-extension or under-

extension.

Platform Vertical Travel Mechanism

A three-bellow airbag was chosen to actuate the vertical travel of the test stand platform. Air

bags are able to easily accommodate high loads as well as a wide range of height changes. Air

bags also have a small footprint when collapsed that does not require extra space for a cylinder

or rod to retract, such as with a hydraulic of pneumatic cylinder. The chosen airbag was capable

of achieving the maximum test stand load of 4454 N (Model no. 9109007, Parker Hannifin Ltd,

Cannock, UK). The airbag was directly mounted to the upper platform and supported using a

trunnion plate at the bottom Figure 2-2. The trunnion changed the compressive loads applied to

the airbag into tensile loads for the test stand's load cell and was designed to have a 1:1 ratio of

compressive load to tensile load. The length of the cam follower channel was designed in

combination with the height-actuating mechanism in order to provide sufficient travel range to

extend within desired height limits and prevent damage to the mechanism or airbag. Row unit

design and its integration to a planter tool bar was studied and it was estimated that vertical

travel of the row unit with respect to the planter toolbar would typically be ± 152.4 mm from the

row unit's normal operating height. Therefore, the test stand incorporated a height change

capability of ± 152 mm from level operating condition, or a total height change capacity of 304

mm. The scissor arms also incorporated a bearing in the center of the arms to link them together

which maintains the geometry of the mechanism during platform vertical travel. The mechanism

for vertical travel of the platform was used to set the row unit height for appropriate operation

during the simulation of field operating scenarios.
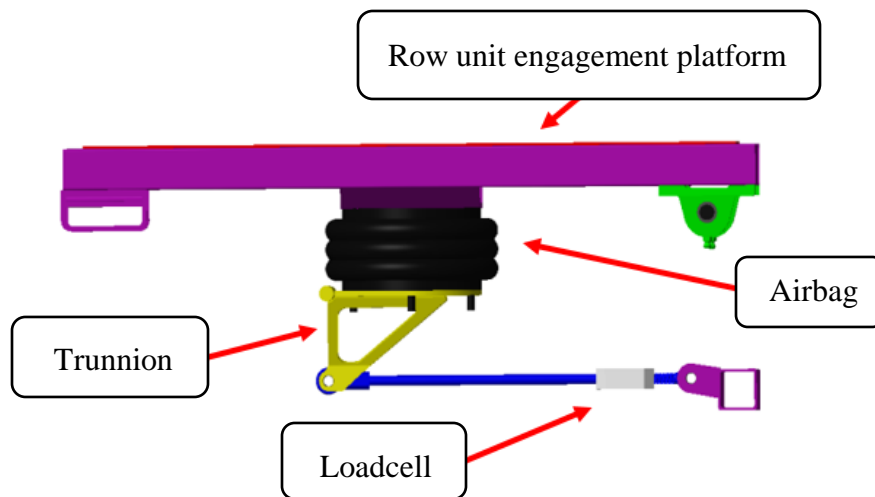
Figure 2-2 Airbag load and height actuation mechanism

Opening Disc Loading Mechanism

A cut-out section was centered on one end of the platform for the opening discs to protrude

through and engage the disc load mechanism. The cutout allowed for common disc depth

settings to be realized during the testing process. The platform was 355.6 mm x 863.6 mm and

the cutout was 38.1 mm x 469.9 mm. The cutout in the platform allowed for the row unit's

opening discs to be set to a typical planting depth of 38.1 to 50.8 mm. The height of the disc

11

load mechanism was adjusted to match the row unit depth setting by slots located on the disc

load mechanism under the platform, Figure 2-3.
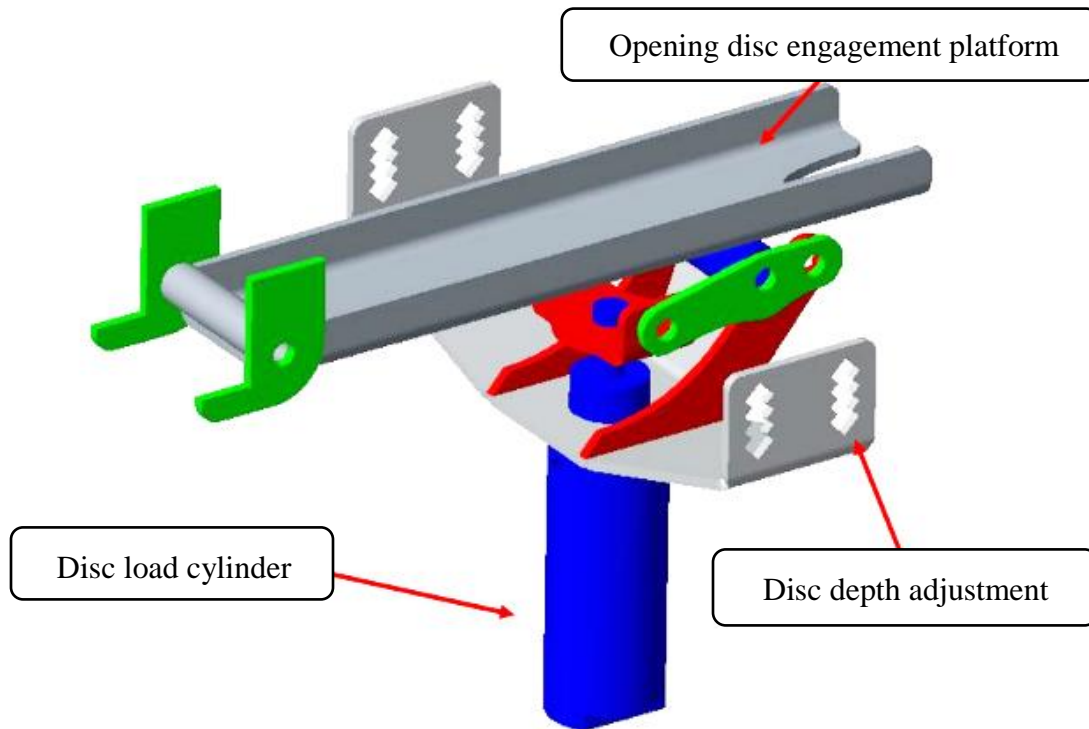
Figure 2-3 Disc load mechanism

The disc load application mechanism was attached to the underside of the upper platform so that

any load applied by it was measured through the platform height/load actuation mechanism and

airbag trunnion/loadcell. The disc load application mechanism consisted of a steel, cantilever

channel with a fixed pivot on one end and an air cylinder on the other end. The disc load air

cylinder applied load to the channel through a roller and linkage mechanism to account for

movement in the channel geometry when it raises or lowers.

The air cylinder was capable of producing a force of 1668 N (Part no. F32020DN, Automation

Direct, Cumming, GA, USA). Real-time planting data (Sylvester et al., 2016) exhibited that disc

loading variability typically occurred during soil EC changes; varying planting speeds and; soil

texture/terrain deviations on headlands and within the field. As a result, the disc loading

mechanism was designed to input varying real-world opening disc loading that occurs during

field operation. Application of varying disc load will change the load distribution between the

opening discs and gauge wheels (assuming closing wheel load is approximately uniform) thus

actuating the downforce control system to maintain target gauge wheel loading. The closing

wheel load is assumed to be uniform because the wheels are spring-loaded and the spring tension

does not change throughout any lab testing. The notch-setting mechanism for closing wheel load

is shown in Figure 2-4 below.

Figure 2-4 Closing wheel notch settings for adjustment of closing wheel load

Sizing and Selection of Control Components

The pneumatic components used within the downforce test stand were sized to apply loads that matched the loading determined from field data. To apply and release air pressure from the test stand's airbag and disc load cylinder, pneumatic solenoid valves (Part no. DVD-2BC4A-24D & DVP-2DC3F-24D, Automation Direct, Cumming, GA, USA) were used. The pneumatic solenoid valves controlled the increase and decrease in load at the pneumatic loading components. The valves were sized and selected for the two pneumatic circuits on the test stand, the airbag and disc cylinder circuits, based on their required flow rates, Appendix A. The airbag load circuit requires a larger valve whereas the disc load circuit requires a smaller valve.

The stand incorporates two valves for each pneumatic load component (the disc load cylinder and height actuating airbag), making for a total of four pneumatic solenoid valves to operate the test stand. Supplying pressurized air to the inlet pneumatic solenoid valves (load increasing) were two pressure regulators, one for the disc load cylinder and the other for the airbag load circuit, Figure 2-5. The two air pressure regulators/water filters (Part no. AFR-4433-MD & AFR 2233, Automation Direct, Cumming, GA, USA) supplied the airbag valve with a maximum of 550 kpa while the pneumatic cylinder valve for loading the opening discs received a maximum of 827 kpa. The two separate pressure regulators set the maximum pressure supplied to each load system based on the pressure needed to achieve maximum loading. By limiting the maximum supplied air pressure to the load increasing valves, damage to the test stand is prevented. Air pressure to the pneumatic system was supplied by an air supply at 896 kpa and an in-line compressed air accumulator with a safety pressure relief valve. The air accumulator was installed in-line just before the pressure regulators to ensure that loss of airflow did not occur

during peak use. At peak use, a maximum flow requirement of 16.67 L/min of compressed

airflow is needed to supply two test stands that are changing height and disc load concurrently.
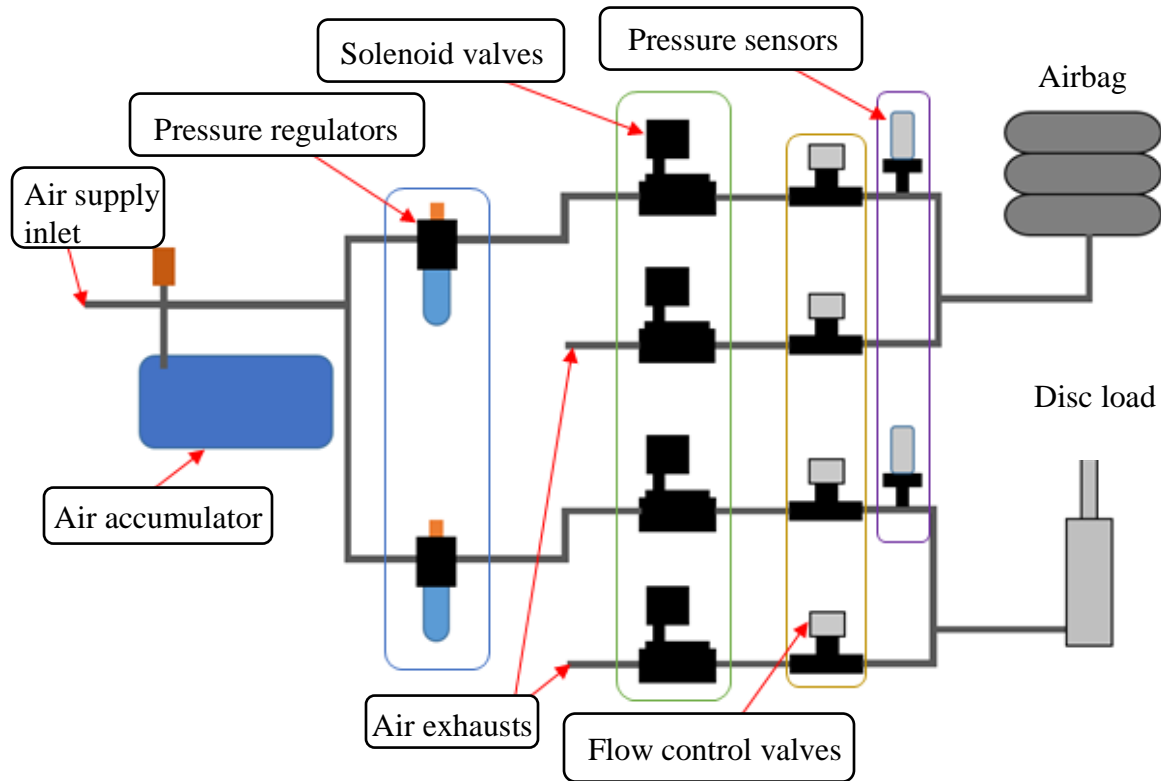
Figure 2-5 Schematics of the pneumatic actuation system

The flow control valves, (Part no. FVU12 & FVU14, Automation Direct, Cumming, GA, USA)

compensate for the different pressure differentials that are across the load increasing and

decreasing valves, Figure 2-5. By adjusting the flow control valves, the flow rates of the

increasing and decreasing valves are synchronized, as close as possible, to reduce timing effects

that must be countered by the electrical control system. The synchronized air flow rates

decreased the complexity of the electrical control system to provide more uniform results. At the

load-increasing valve, pressure at the valve inlet is at the regulated supply pressure and on the

valve outlet the pressure is at the current pressure in the pneumatic load component. At the load-decreasing valve, pressure is at atmospheric on the exhaust side and the inlet side of the valve is at the current pressure in the pneumatic load component.

Data Collection and Test Stand Control

A custom LabVIEW program (Labview, 2014) was developed to operate the downforce test stand's pneumatic valves and record data from the test stand and row unit sensors using a National Instruments (NI) CRio Chassis. On the test stand, the total downforce load was measured using a S-type load cell (Part no. 1631-03C, PCB piezotronics, Depew, NY, USA). Gage wheel load was measured through a 9810 N load cell (Part no. J4-1000, Fliegel, AgrarTechnic GmbH, Mühldorf, Germany) mounted on the planter row unit. Row unit hydraulic pressure and hydraulic supply pressure were measured through two hydraulic pressure sensors, (HAD 844L-A-0250-161, Hydac, Glendale Heights, IL, USA). Opening disc cylinder pressure and airbag pressure were measured through two pneumatic pressure sensors, (Part no. 1502881EZ100PSIG, PCB Piezotronics, Depew, NY, USA). Instantaneous test stand height was measured using an ultrasonic distance sensor, (Part no. UR18.DA0-11119994, Baumer, Southington, CT, USA). Among all the sensors, the gauge wheel load cell and one hydraulic oil pressure sensor were located on the planter row unit itself. To obtain the PWM duty cycle sent from the planter ECU to the automatic downforce hydraulic control block, the ECU signal wire was tapped and the signal sent to the NI 9403 module. The LabVIEW program counts the time that the PWM signal is high vs. low to calculate the duty cycle. The PWM signal produced by the planter ECU represents the automatic downforce control system's output. Several NI C-series modules (NI 9476, 9205, 9221, 9205, 9203) in the CRio chassis provided digital and analog inputs and outputs to interface with the various valves and sensors. The LabVIEW

program read control commands from a *.txt file, henceforth referred to as a simulation file, to

actuate desired disc loads through the disc loading mechanism and platform height through the

platform height control mechanism. The program read the simulation file containing target

values of disc load and platform height, parsed the data fields, and sent it to the corresponding

control loops. The control loops used the simulation file data as a target load or height setting

while reading pressure transducer and ultrasonic sensor data for current load of the disc cylinder

and current height of the test stand, respectively. If the difference between the set value and

actual value was above a set threshold, the control loop would adjust the pneumatic component

up or down to achieve the desired load setting. A flow diagram of the program's operation is

outlined in Figure 2-6.
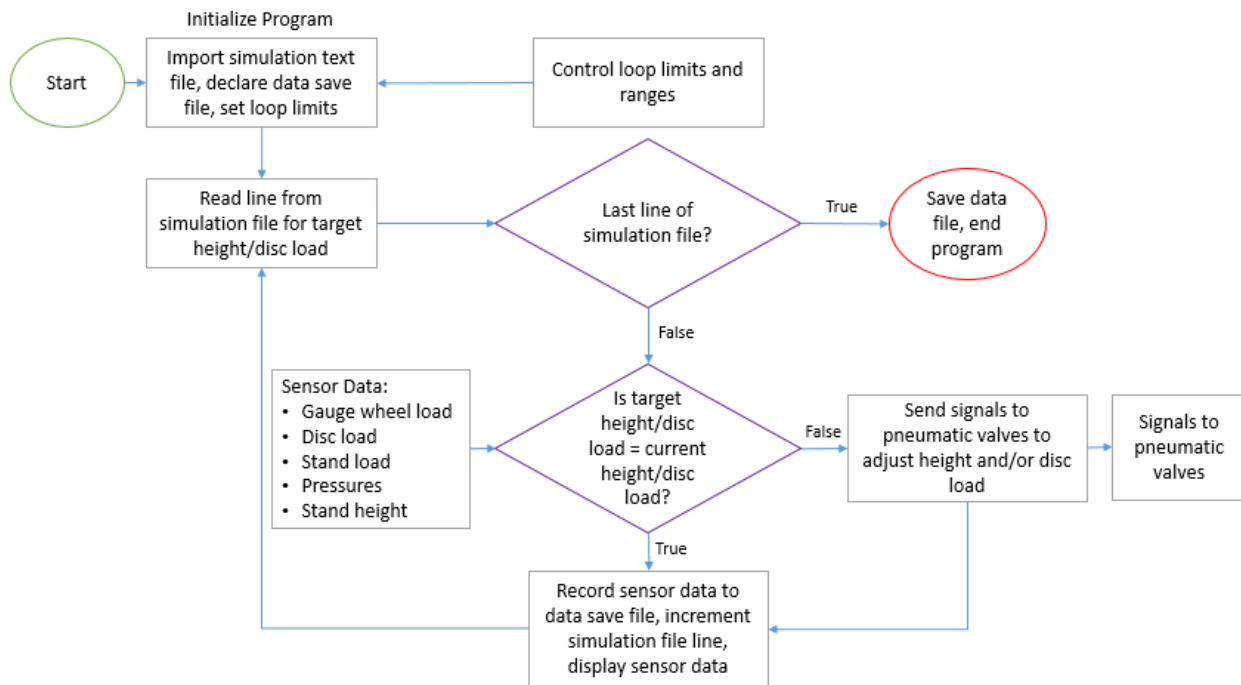
Figure 2-6 – LabVIEW program logic flow diagram

The program included a main data display screen to observe real-time critical parameters during

test stand operation. Real-time values displayed were total stand load, disc load, gage wheel

load, press wheel load setting, hydraulic oil pressure in several key locations, and the duty cycle

of the planter's ECU Pulse Width Modulation (PWM) output that controlled the planter's

hydraulic downforce. The screen also contains operator controls to start and stop downforce test

simulations, Figure 2-7.
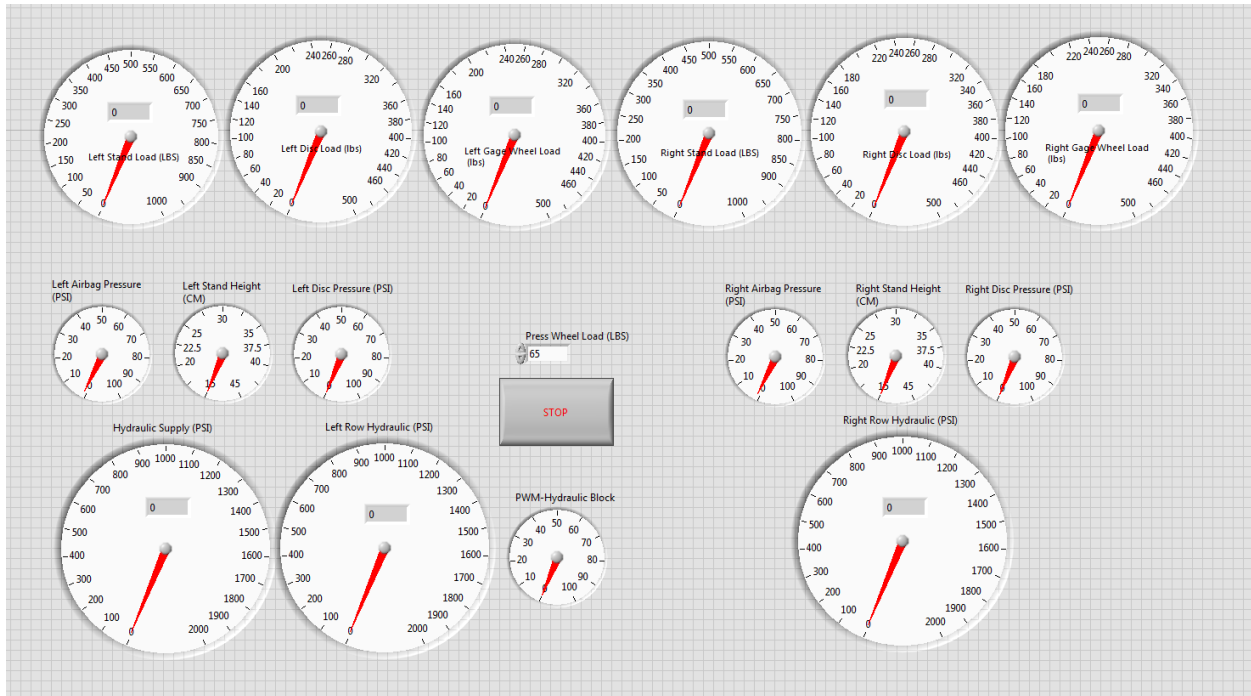
Figure 2-7 Screen view of LabVIEW downforce test stand control program showing various sensor readouts and controls

Downforce Test Stand Verification

To verify the operational capabilities of the developed downforce test stand, multiple verification

scenarios were tested and replicated three times. These scenarios recorded the accuracy and

settling time that the test stand achieved when raising or lowering the platform and when loading

and unloading the opening discs. During these evaluation tests, the row unit was set to a

constant downforce output to load the test stand.

Disc Loading Control Verification

The first evaluation tests were pulsing the opening disc pneumatic valves once per second to gain

a load change per pulse curve with respect to pressure in the disc cylinder. A linear regression

equation was fitted between the pneumatic cylinder pressure and the load applied to the opening

discs, Figure 2-8. The regression equation was utilized in the LabVIEW program to determine

the number of valve pulses that are required to change the set disc loading from one set point to

another within the disc cylinder's operating pressure range. Although a hysteresis effect was

present, due to the variable pressure differentials across the solenoid valves affecting the airflow

rate, the maximum error produced by this effect is 14%, or $\pm$ 177 N and is considered acceptable.

However, it had an effect only on the control system in terms of pulses needed for achieving

target disc loading.
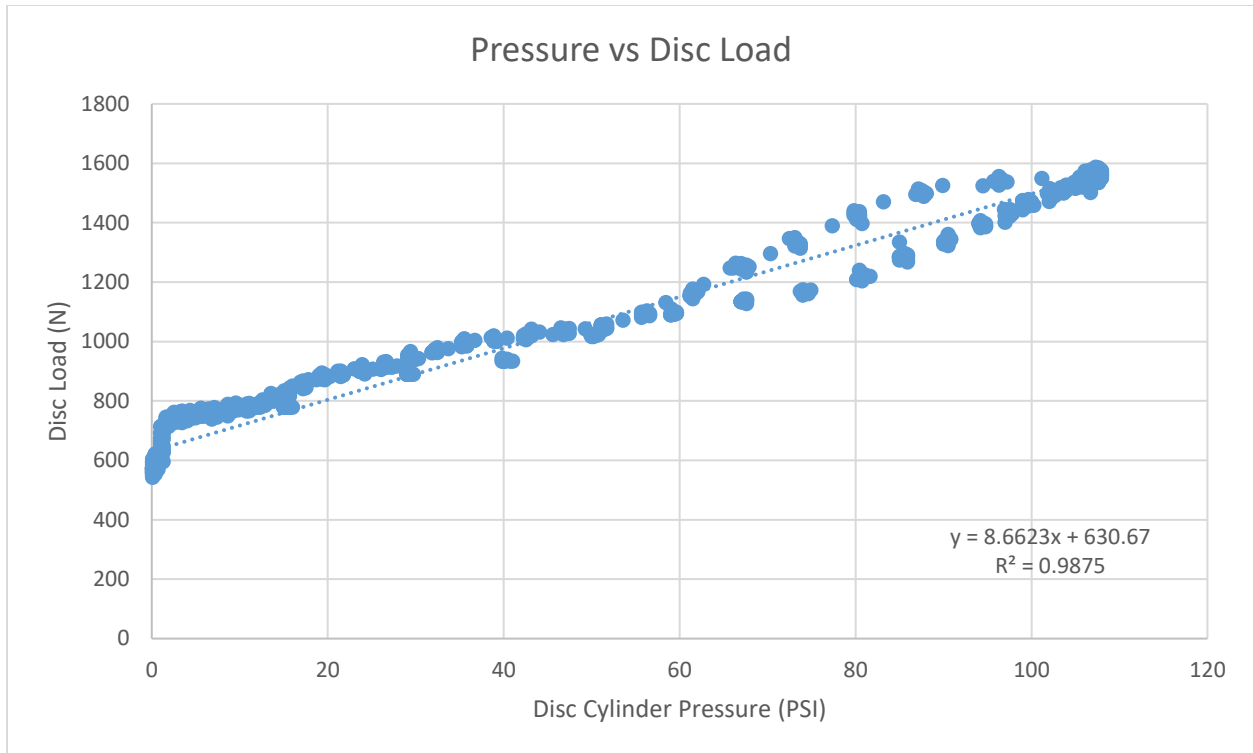
Figure 2-8 Disc cylinder pressure and its relation to disc load

The test, Figure 2-9, also allowed for measurement of the opening disc load system's average

settling time. The settling time for the opening disc system was defined as the time it takes for a

signal to be sent from the LabVIEW program to the time when the change occurred. On an

average, the disc load mechanism was able to achieve a settling time of 0.2 seconds when

loading or unloading the disc within the typical operating range of 667 to 7573 N of disc load,

Figure 2-9. The control and pneumatic system response was deemed appropriate to send disc

loading simulation control signals to study control system response under dynamic conditions.
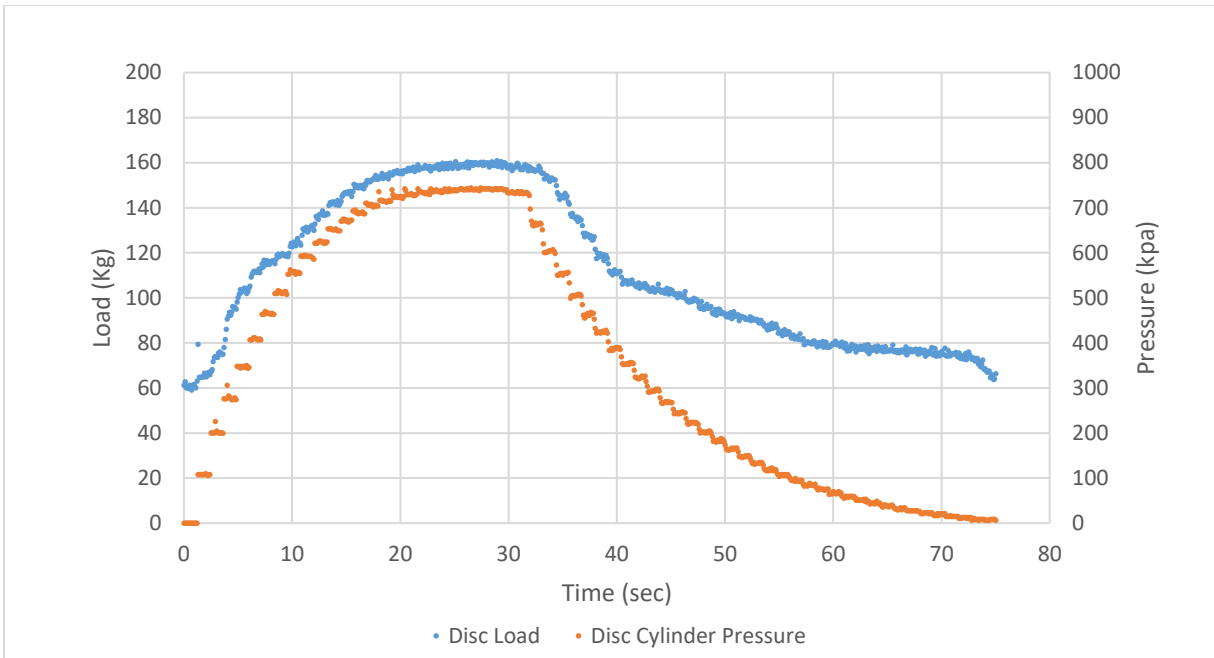
Figure 2-9 – Disc load actuation during pressure step changes

Test stand Vertical Travel Mechanism Verification

Three replicated tests were conducted that raised the planter test stand platform at 1.0 cm, 1.5 cm and 2.0 cm increments. The tests started with the platform at its middle height position, then it was raised up 152 mm, lowered down 304 mm, and raised back up 152 mm to the middle position. The tests demonstrated that the control and actuation system could accurately change platform height to within 0.5 cm of the target height during vertical travel. The vertical travel tests also allowed for the testing of the stand's settling time for height changes as well. Results indicated that the test stand's settling time for height change commands, on average, was always within 0.33 seconds, Figure 2-10. The settling time of the test stand's vertical travel system is defined as the time for a signal to be sent from the LabVIEW program to the time when the height change began to occur.
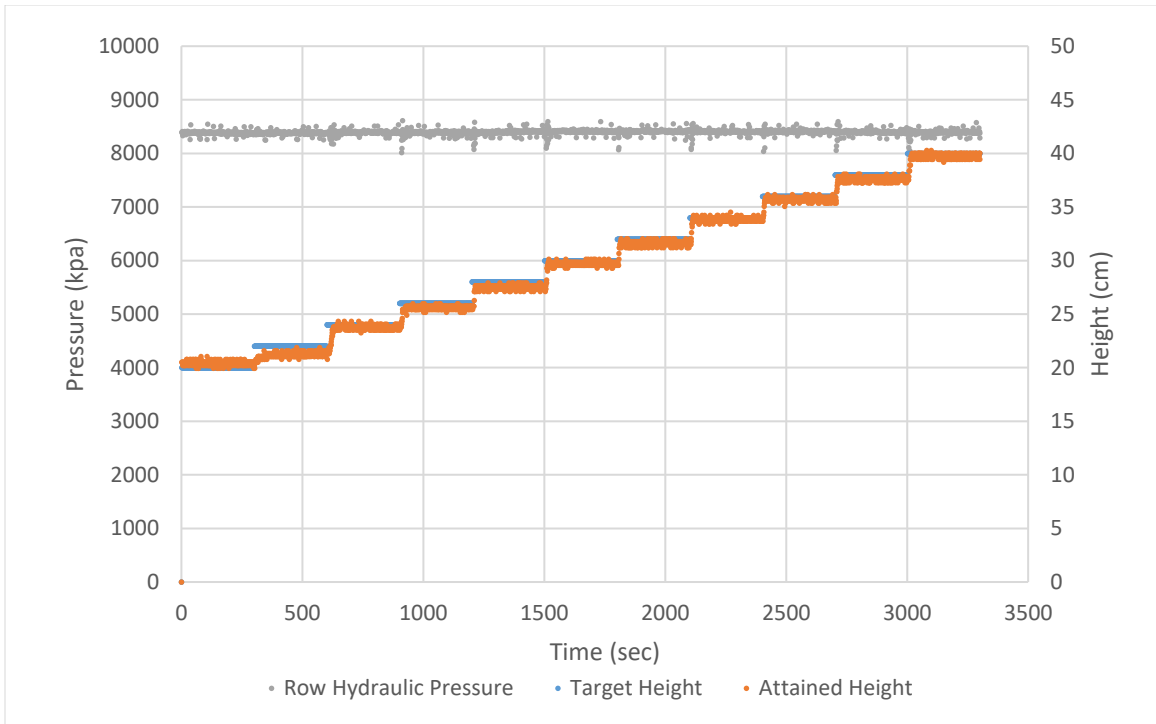
Figure 2-10 Response and accuracy of test stand vertical travel during 2 cm step changes

Field Data Simulations

After evaluating the operational capabilities of the downforce test stand, several scenarios were

chosen from operational field data to be simulated and analyzed on the downforce test stand for

automatic downforce system evaluation. The scenarios were chosen with varying and dynamic

opening disc load variability, which would change the gauge wheel/disc load distribution and

demand automatic downforce system actuation. The field data included information on real-time

gauge wheel load and hydraulic pressure. To derive real-time disc load, it was assumed that the

total downforce applied is equivalent to the sum of gauge wheel load, disc load and closing

wheel load. Total downforce load is the sum of row unit weight and applied hydraulic load,

Figure 2-11.

22
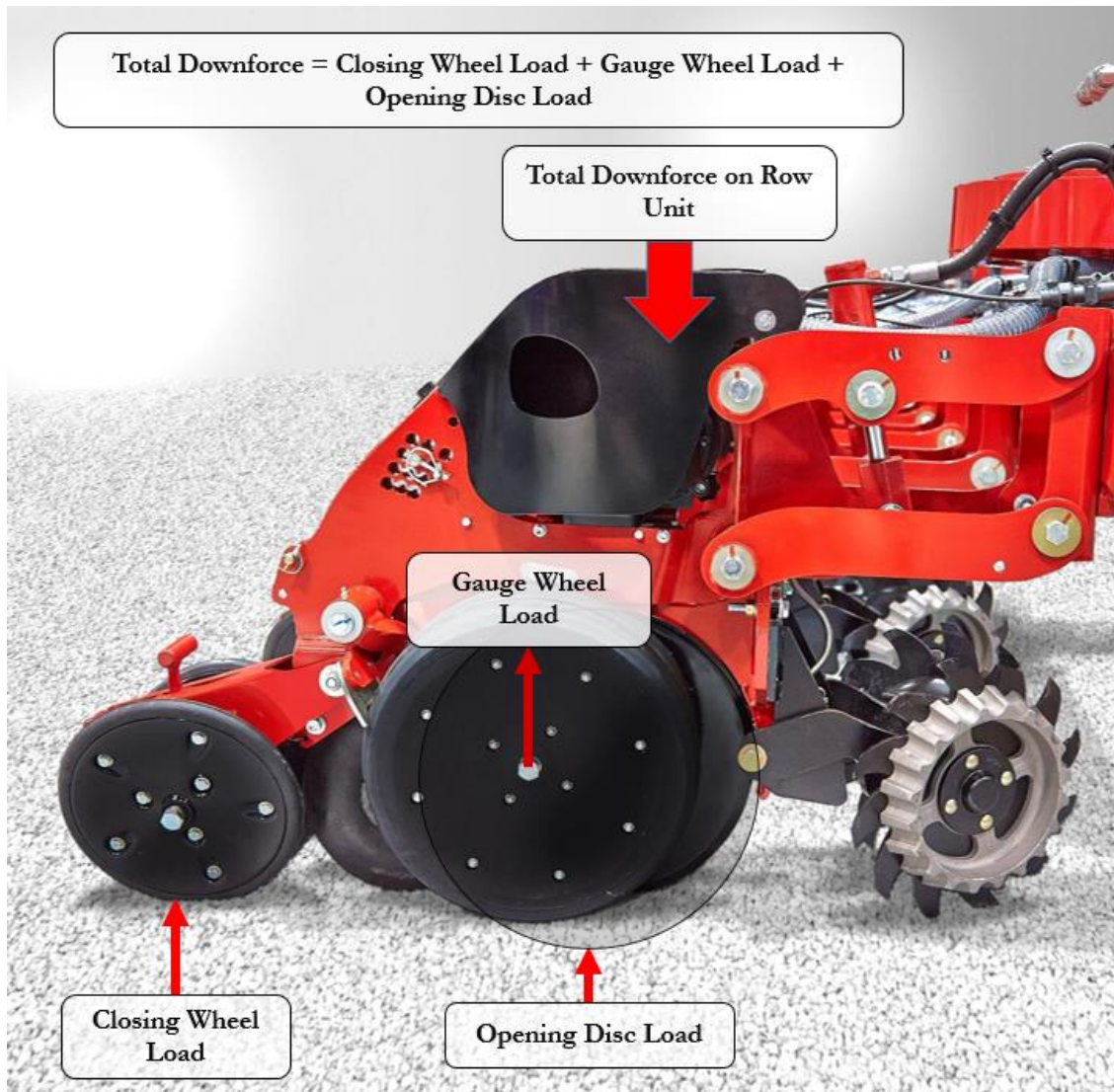
Figure 2-11 Illustration of critical planter component loading forces

To collect the total downforce applied at different hydraulic pressures, the downforce test stand

was set to maintain a constant row unit ride height while the hydraulic pressure output was

changed using the planter's diagnostic screen. A linear regression was fitted between row unit

cylinder hydraulic pressure and total downforce, Figure 2-12. The results show the relationship

between the applied row unit hydraulic pressure and the total load applied and the intercept of

the equation represents the weight of the row unit. The regression equation was used to calculate

total downforce from real-time hydraulic pressure data during simulation tests.
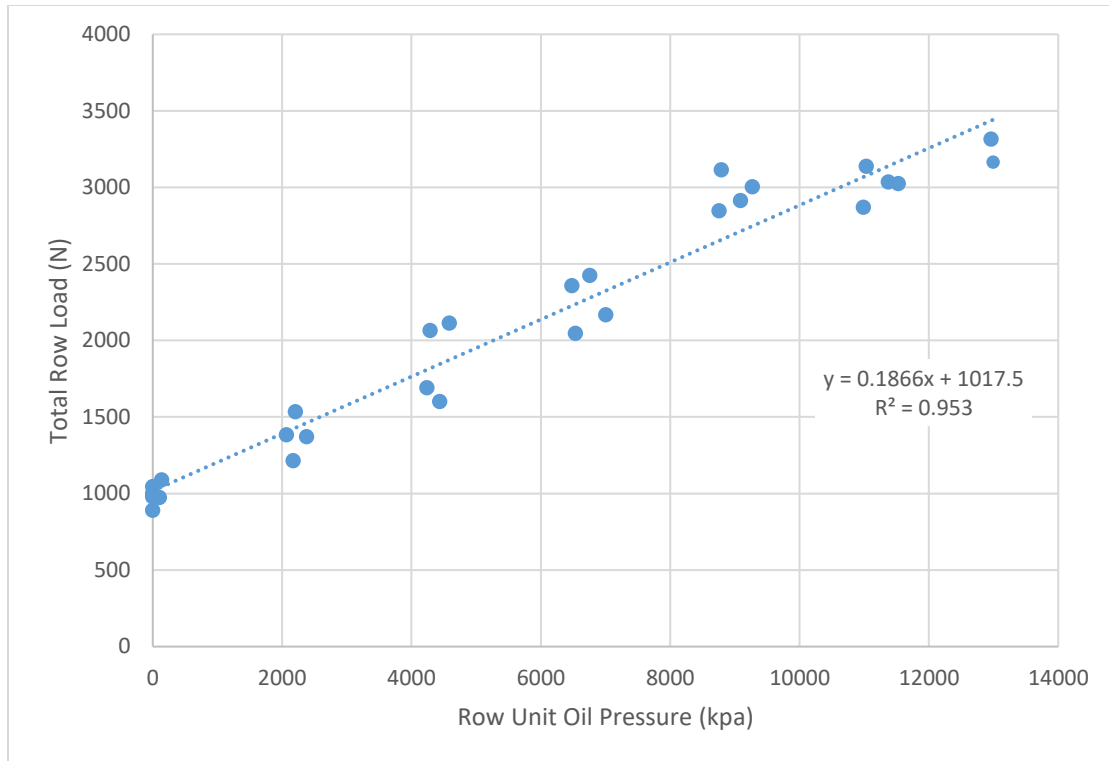
Figure 2-12 Relationship between applied row unit hydraulic cylinder pressure and total downforce on row unit

Next, to collect data that represents the closing wheel load in each respective notch setting, the downforce test stand was set to a constant height with no applied disc loading and the planter was set to a constant hydraulic downforce pressure. The closing wheel load notch was changed between settings one thru four to produce the following forces in each setting respectively; 294, 383, 500, and 608 N. The simulation test files were created by calculating total downforce using real-time hydraulic pressure from field data and the hydraulic pressure versus total downforce regression curve, the calculated real-time disc load by subtracting real-time gauge wheel load from field data, and closing wheel load (notch two was used in the field data) from total downforce, to calculate the real-time disc loading that occurred in the recorded field data. The previous is represented by the following equation:

$$Disc\ Load\ (Kg)\ =\ (0.019 * Oil\ Pressure(Kpa) + 103.72) -$$

$$(Closing\ wheel\ load\ (Kg)) -\ Gauge\ wheel\ load\ (Kg)$$

Experimental Design

Three field scenarios were selected with the planter travelling at 7.2, 9.7, and 12 kph, henceforth referred to as S1, S2, and S3 "Disc loading at Planting speeds" in order to quantify the automatic downforce system response and accuracy at maintaining target gauge wheel load during varying planting speeds. Figure 2-13 shows the soil electrical conductivity (EC) map, with test strip areas labeled, of the field where the real-time planting data was recorded that was used for generating the simulation test files. The simulation scenarios selected were from side-by-side data strips planted on soil with approximately the same soil EC, and moisture content. The selected scenario with different planting speeds provided data to deduce disc load variability and an understanding of the control system's ability to consistently maintain target gauge wheel load within the target range. The second set of simulation scenarios were from data strips representing a planter traversing from a section of the field with a heavier soil texture to a lighter soil texture represented by changes in soil EC. Data from two planting speeds of 7.2 kph and 9.7 kph with the planter moving through a varying soil texture were selected to generate simulation text files, henceforth referred to as S4 and S5 respectively "Disc loading on Varying Soil Textures", Figure 2-13.

Finally, the third simulation scenario was selected with the planter operating on a field edge with a rocky/hard clay soil that produced highly variable disc loading. The planter was operating at

9.7 kph and the simulation will be referred as S6, "Disc Loading on Rocky-Hard soil Zone",
Figure 2-13.

Response time of the control system was evaluated by selecting the following simulated
scenarios:

a) 223 N disc load change within S4, "Disc loading on Varying Soil Texture"
scenario;

b) 446 N disc load change within S5, "Disc loading on Varying Soil Texture"
scenario and;

c) 667 N disc load change within S6, "Disc Loading on Rocky-Hard soil Zone"
scenario.

These simulated scenarios provided an understanding of the downforce system's response during
different disc loading transitions and the downforce system's ability to maintain target gauge
wheel load during such conditions in the field. For all tests, the controller was set to maintain a
target gauge wheel loading of 379 N. During the collection of field data, no data was recorded
with row unit vertical travel, so for all of the tests conducted for this study the height of the test
stand was held constant.
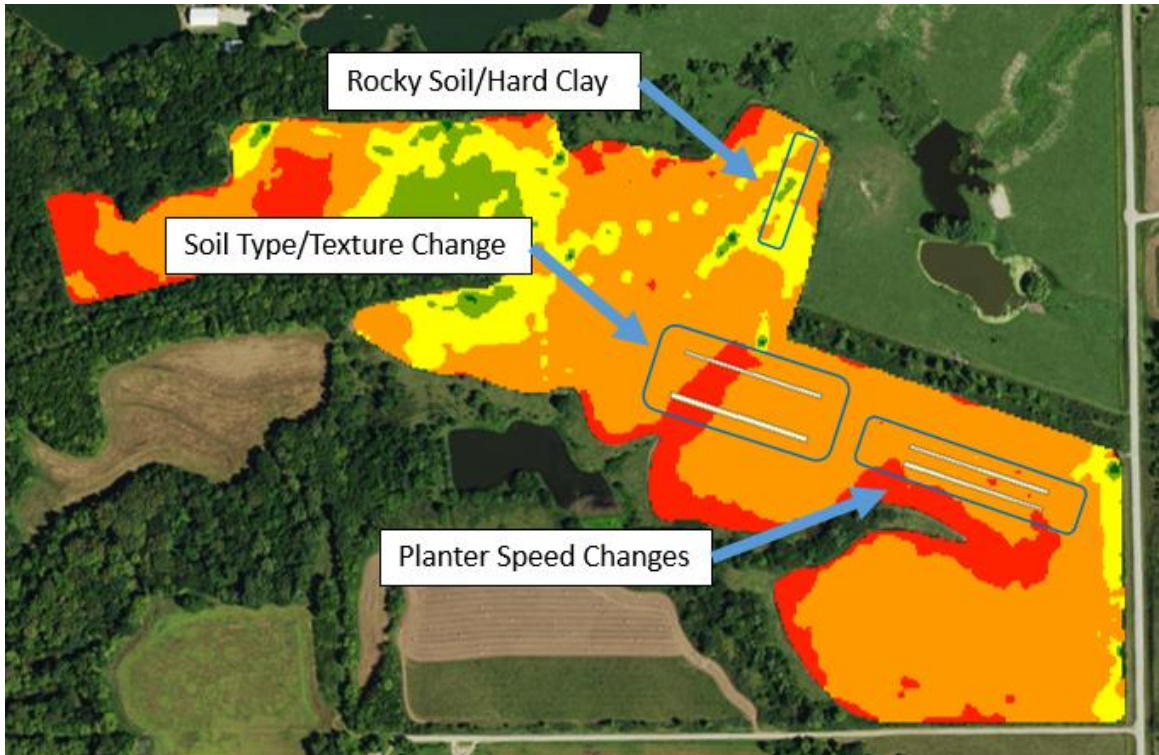
Figure 2-13 Field used for simulation data extraction

Data Analysis

Real-time gauge wheel load, from our simulated scenarios, was analyzed to gather the accuracy and response of the automatic downforce control system. Data was analyzed to quantify the percent time that the gauge wheel load was maintained within ranges of ± 89, ±156, and ±223 N of the target gauge wheel load setting by the automatic downforce controller. These ranges were chosen to represent three levels of downforce operation, selecting a range that describes how well the downforce system would work in a particular field would be dependent on a particular producer's preference. The response time was the difference in time from when the gauge wheel load went outside the desired ±223 N range due to dynamic disc load deviation, and the time

when the gauge wheel load returned within ±223 N of target load. To determine the automatic

downforce controller's ability to respond to different disc load variations, three disc load change

events were selected. The selected disc load change events occurred during the speed

simulations, soil type change simulations and the headlands hard clay/rocky simulation. The

events represent disc load changes of 223, 412, and 677 N.

Results and Discussion

The results for each scenario were evaluated to quantify the effects of speed and soil texture on

downforce system operation and response. For each scenario, the percent time of each test that

the planter remained within a target gauge wheel load range was calculated. Also calculated was

the response time of the automatic downforce system to several disc load change events.

Disc loading at Planting speeds Scenario

Results for S1, S2, and S3 indicated that the downforce control system maintained target gauge

wheel load within ±89, ±156, and ±223 N for an average of 72%, 92%, and 99% of the 7.2 kph

test respectively, Figure 2-14. Similar results were observed for simulation of the planter

operating at 9.7 kph where load was within target ranges of ±89, ±156, and ±223 N for an

average of 61.71, 88.68, and 99.00% of the test, respectively, Figure 2-15, and 12 kph, where

load was within target ranges of ±89, ±156, and ±223 N for an average of 89.02, 99.86, and

100% of the test, respectively, Figure 2-16. The results suggested that the control system could

maintain target gauge wheel loads within tighter ranges for a longer duration of time with the

planter operating at higher speeds, Table 2-1. Although, from a producer perspective, gauge

wheel load within ±223 N of target may be satisfactory. If the goal is to maintain a tighter range,

28

such as ±156 N, then future work needs to be conducted to optimize the control system response with varying speeds.
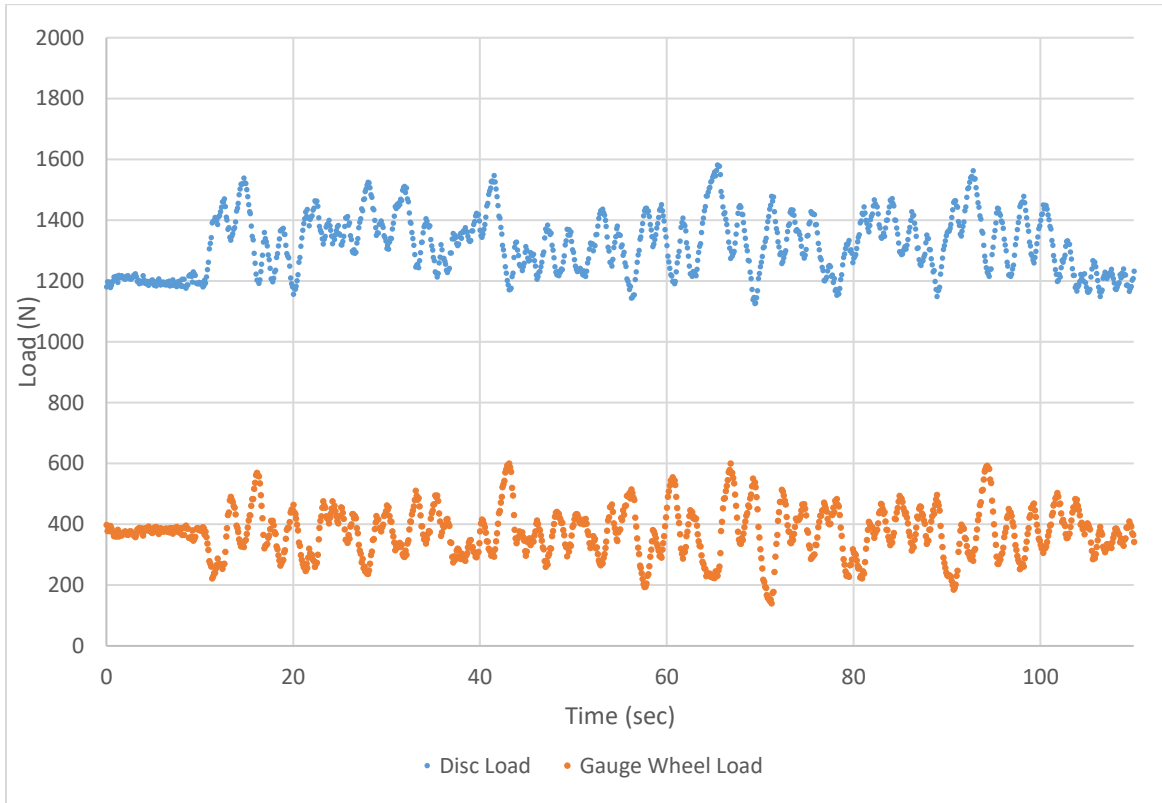
Figure 2-14– S1 simulation of planter operating at 7.2 kph
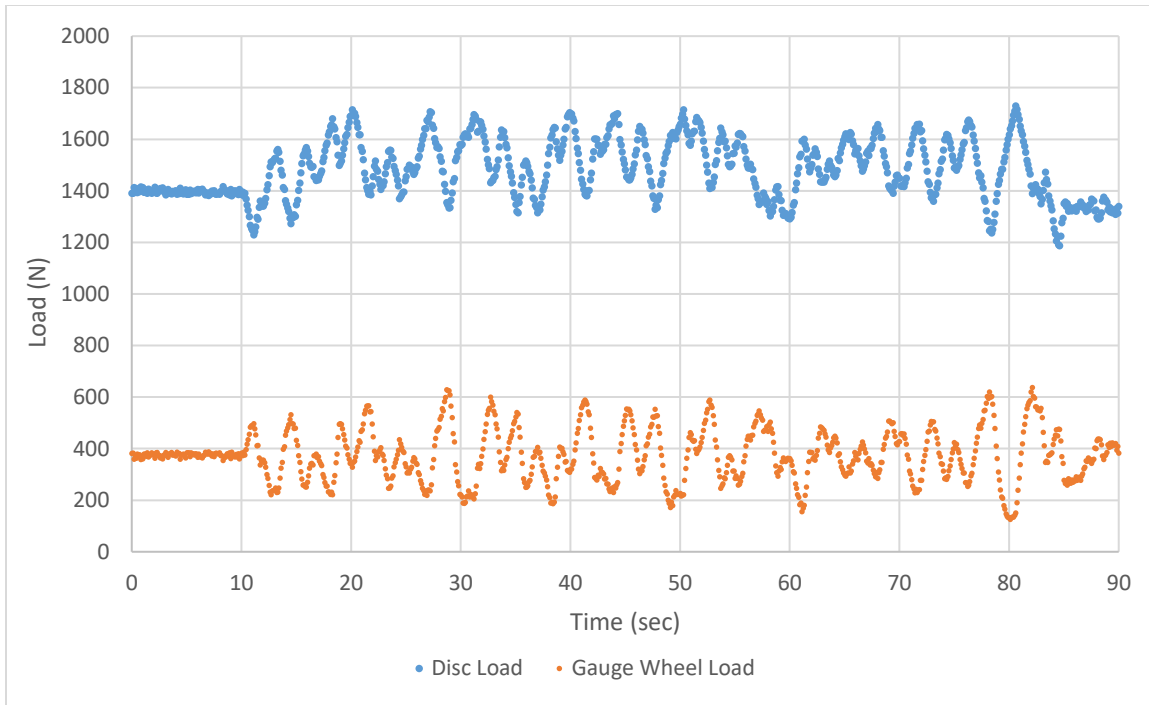
Figure 2-15– S2 Simulation of planter operating at 9.7 kph
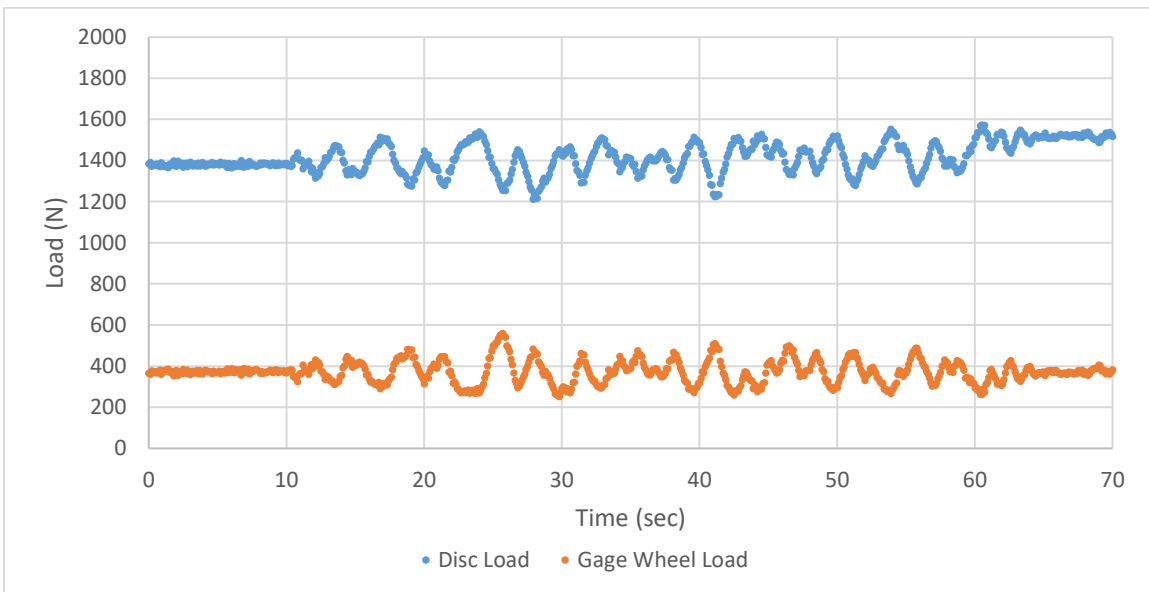
Figure 2-16– S3 Simulation of planter operating at 12 kph

30

Table 2-1 Summary of the planter's ability to maintain target gauge wheel load during simulated scenarios

Simulation Scenario	Percent of test time within ranges		
	±89 N	±156 N	±223 N
S1	72%	92%	99%
S2	62%	89%	99%
S3	89%	100%	100%
S4	77%	94%	100%
S5	80%	90%	96%
S6	60%	847%	94%

Disc loading on Varying Soil Texture Scenario

The results for the S4 and S5 simulation tests indicated that the automatic downforce controller maintained gauge wheel load within ±89, ±156, and ±223 N of target load for 77%, 94%, and 100% of the test, respectively with the planter traveling at 9.7 kph, Figure 2-18. Whereas at 7.2 kph, the planter maintained gauge wheel load within ±89, ±156, and ±223 N of target gauge wheel load for 80%, 90%, and 96% of the test, respectively, Figure 2-17. The simulation results exhibited that the planter, when traversing through varying soil textures, had disc load variations of larger magnitude thus creating a greater control demand.
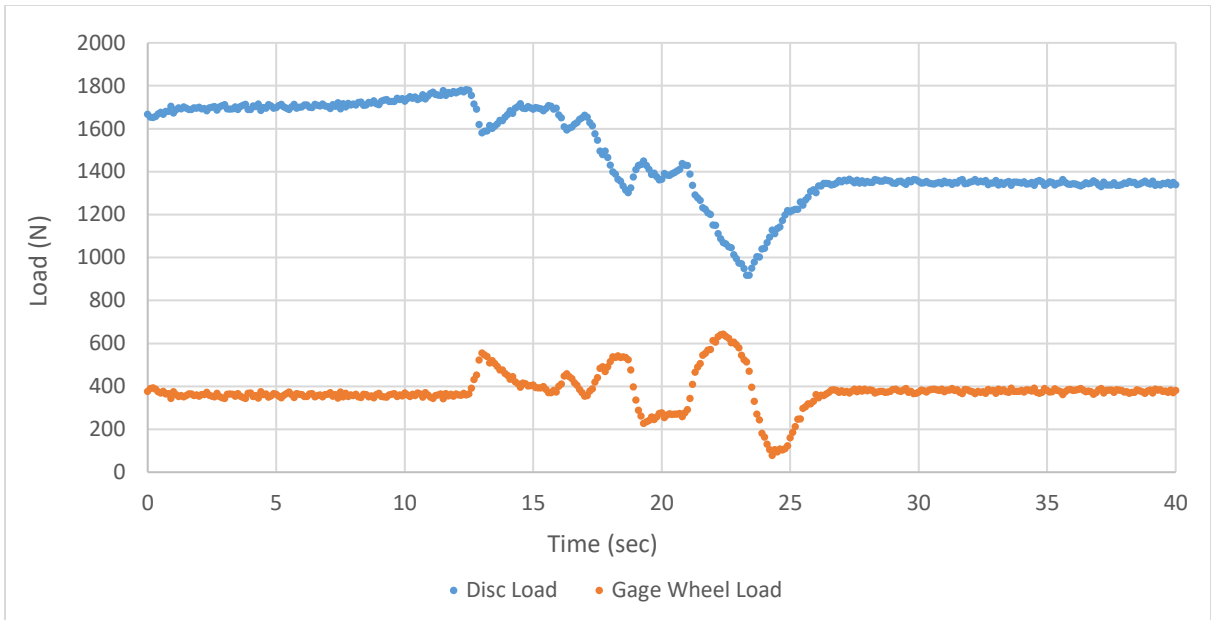
Figure 2-17– S4 Simulation results of planter experiencing a soil type/texture change at 7.2 kph
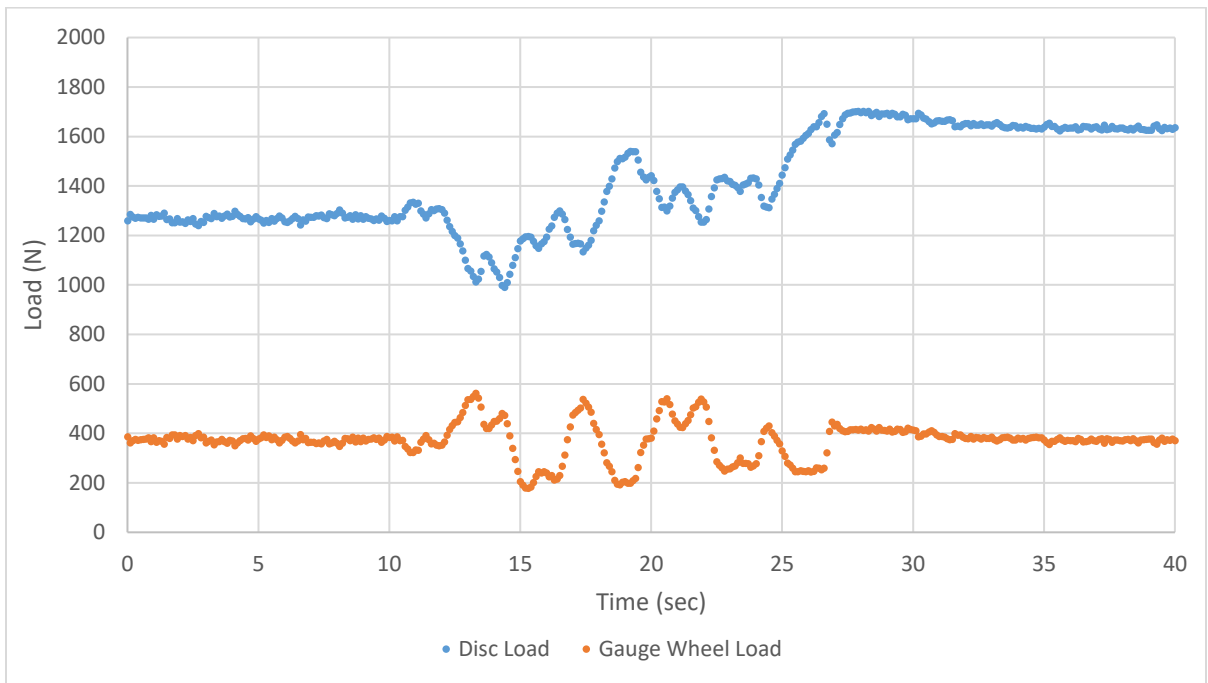
Figure 2-18– S5 Simulation of planter experiencing a soil type change at 9.7 kph

32

Disc Loading on Rocky-Hard soil Zone Scenario

The simulation conducted representing a planter crossing through a field's headlands that contained a hard/packed clay with some rocks indicated that the planter's automatic downforce control system maintained gauge wheel loading within ± 89, ±156, and ±223 N of the target load for 60%, 84%, and 94% of the test, respectively, Figure 2-19.
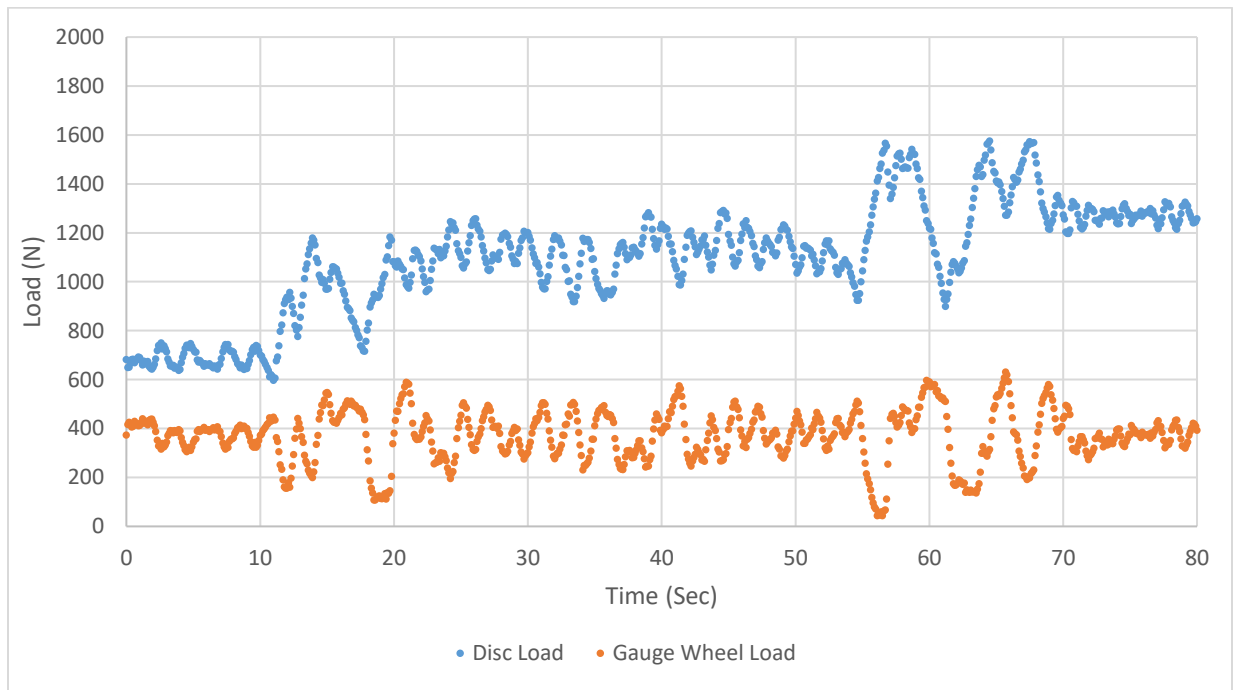
Figure 2-19– S6 Simulation results of planter experiencing a headland with a hard, rocky clay

Overall, during the scenarios representing normal field operations, the speed and soil texture simulations, the gauge wheel load was maintained within ±223 N of the target gauge wheel load setting of 373 N for at least 95% of the time. When a soil type change did not occur, i.e. the disc load average was not changing, the planter maintained gauge wheel loading within ±223 N for at least 99% of the simulation. From analysis of the simulation data, it can be seen that the speed

of a planter has an effect on the dynamic loading that occurs on a planter's opening discs. The

oscillations of the disc loading appear to decrease with speed which could be due to the row

unit's momentum helping the opening discs slice through the soil Figures 2-14 thru 2-16. This

could lead to the need for a more aggressive automatic downforce control system at slower

speeds, and a less aggressive automatic downforce control system at higher speeds. By changing

the "aggressiveness" of the automatic downforce system with speed, the over and under

application of downforce can be minimized to ensure a consistent seeding depth.

During disc load change events of 223 N and 412 N, the gauge wheel loading was maintained

within a range of ±223 N throughout the event, Table 2-2. During a large disc load variation of

677 N, the gauge wheel load was out of a ±223 N range for, on average, 1.3 seconds, Table 2-2.

This large disc load variation event occurred during the hard clay/rocky headlands situation and

the results suggest that, for most of a typical field, the automatic downforce controller would be

able to maintain the gauge wheel load to within ±223 N of the target load. The response times

that are not listed in Table 2-2 represent events where the planter's downforce was always within

an acceptable range throughout the event.

Table 2-2 Average downforce control system response time during different disc load change events

Disc Load Change Event (N)	Disc Load Change (N)	Disc Load Event Length (sec)	Response time (sec)
223	1246 to 1432	1 second	-
445	1707 to 1295	3.1 seconds	-
667	912 to 1589	2.2 seconds	1.3

The selected field simulations are representative of what will occur in a typical field for nearly all of the planting operation. When the downforce system was simulated as passing through severe field conditions, such as a hard clay/rocky headland, the automatic downforce controller was able to maintain gauge wheel loading within ±223 N for over 94% of the simulation. Because the planter was able to maintain gauge wheel loading within the target range of ±223 N during all field conditions, this system would be able to provide proper seeding depth throughout an entire field.

Conclusion

With the development of a lab-based planter evaluation stand, the row unit's downforce distribution was evaluated using real-time field data simulations. The test stand setup provided an opportunity to study the relationship between changes in disc loading and automatic downforce controller response. Tests using real-world data can be conducted in a repeatable manner to evaluate current production automatic downforce systems and make changes to enhance that system's response and accuracy. The main conclusions of this study were:

1. The test stand was able to conduct planter downforce control system evaluation using real-word field data.

2. The test planter's automatic downforce control system maintained the target gauge wheel load setting of 373±223 N for more than 94% of the time during all simulations.

3. The downforce control system was able to manage gauge wheel load with disc load variations up to 667 N within 1.3 sec.

Chapter 3 - Performance of a Planter with Electronic Drive Singulation Seed Metering System during Simulated Planting Scenarios

In recent years, there has been a push for faster planting speeds to increase productivity and reduce the amount of time spent in the field. Producers in areas that experience varied weather conditions that can limit the amount of time available for planting will benefit from faster planting speeds. If weather is varied, adequate soil moisture may only exist for a short period of time, reducing the length of the opportune planting season. Corn germinates and emerges best when adequate soil moisture is present, therefore if planting can be accomplished faster, producers can increase their yield potential during short planting seasons, (Nielsen, 2004). Faster planting speeds also benefit larger scale operations, which have many acres to plant within a small planting season. High speed planting would also allow large scale producers to cover the same amount of acres with less machines, which saves on equipment costs and operating expenses, (Miller et al, 2012; and Staggenborg et al, 2004).

Many classic singulation seed metering [*ASABE Standard S506*] systems were ground driven. These systems are effective at planting because the meter's seed output rate is related to ground speed, (Yeon, 2004). This allows these singulation seed meters to maintain proper seed spacing automatically with tractor ground speed. Studies have shown that maintaining proper seed spacing is important for corn emergence and yield, (Nielsen, 2005). Nielsen's study found that corn spacing variability could directly affect yield. The yield losses caused by the spacing variability was due to interplant competition, (Liu et al., 2004).

Although classic ground driven singulation seed meters can provide proper singulation at slower planting speeds, studies have shown that classic singulating seed metering systems have performance losses at high planting speeds, (Miller at al., 2012; and Taylor et al., 2004). These studies have shown that with increased meter speeds, due to higher seeding rates or higher planting speeds, the meter's singulation decreased and therefore proper plant spacing was not accurately maintained. The impacts of planter type on corn stand uniformity and yield has also been studied by (Liu et al., 2004). Liu found that planters utilizing a vacuum type seed metering system were better suited for higher planting speeds over finger-type planters or air seeders.

To address the issues of classic seed metering systems operated at high speeds, new metering systems with electronic drives have become available. A typical electronic drive singulation seed metering system in use is the Precision Planting vSet meter which features an electronically driven seed meter, (Precision Planting, Tremont, Illinois). Another electronic drive singulation seed metering system is Horsch's Maestro planter which features a seed plate directly driven by an electronic motor and planetary gearbox assembly, (Horsch Maschinen GmbH, Schwandorf, Germany). Also on the market is John Deere's ExactEmerge Row Unit which features an electronically driven singulation seed meter as well as an electronically driven seed belt-brush delivery system, (Deere & Company, Moline, Illinois). The seed plate in these systems is either mounted directly to the electronic motor shaft or is driven using internal gear teeth around the perimeter of the seed plate that mesh with the electric motor. A row control module (RCM) maintains the desired seed plate speed to match the target seeding population and instantaneous ground speed for each row unit individually.

Because of individual metering systems for each row unit, contour compensation and point-row shutoff can be easily implemented through software; without the need to re-configure the entire

planter's drive system. Previously this was accomplished by replacing a traditional planter's ground drive system with one utilizing either hydraulic or electronic drive motors, (Yang, 2015). Planter systems incorporating contour compensation utilize the RCM to control the individual row unit speed and maintain proper seed spacing regardless of toolbar location. Contour farming and point-row shutoff functionalities can potentially increase productivity by reducing the over-planted area of a field; especially in a field with an irregular shape or terraces. (Velandia et al., 2013; and Corn and Soybean Digest, 2013).

Newer electronically driven seed metering systems can potentially increase the performance of a planting system, however little knowledge on the accuracy and response of these systems during varying planting speeds and contours is known. Therefore, the objective of this study was to quantify electric motor accuracy and response, by comparing measured meter speed to target meter speed, during simulated field conditions.

Methodology

Planter setup

A production Horsch Maestro 24.30 SW (24 rows on 30" spacing) planter (Horsch LLC, Mapleton, North Dakota) was utilized with individual electronic drive seed meters. The electronic drive seed meters were linked through an ISOBUS to the planter's display. Controlling the electronic drive seed meter speeds was the Horsch Terminal ME controller display that gathers ground speed data at 10Hz from three radar speed sensors (Radar III, Dickey John Corporation, Minneapolis, Minnesota) mounted on the planter toolbar and chassis. Two of the ground speed radars were located on the left and right end row units of the planter toolbar

with a center radar mounted to the drawbar of the planter chassis. After the Horsch planter's

Terminal ME controller display acquired speed signals from the three ground speed radars, it

produced a signal over the planter ISOBUS to control individual row unit seed metering speeds

via each row's RCM.

During planter operation, the Horsch controller was programmed to compare the speeds from the

left and right radars to the center radar to calculate a speed differential across the planter toolbar.

If this speed differential was less than 0.48 kph, the controller operated in straight-line planting

mode with all electronic drive seed meters at the same speed. If the speed differential was

greater than 0.48 kph, the controller entered into contour farming mode. Contour farming mode

varied electronic seed meter speed at every row unit, based on the speed differential, to maintain

the proper seed spacing on each row during contour farming operations.

A Challenger MT875C tractor (AGCO, Duluth, Georgia) powered the planter's hydraulic and

electrical systems. The corn seed used for these studies was Dekalb Brand DKC48-12RIB

(Monsanto, St. Louis, Missouri) medium round seed. The planter had 21 slot seed plates for

medium round corn seed installed.

 Operator simulations

To determine common in-field operating practices to test under simulated conditions, recorded

planting data was studied from several Kansas fields to determine common in-field speeds

during straight runs, acceleration and deceleration during headland operations, field obstacles,

and traveling along contours. The planting data revealed that some operators preferred to enter

and exit headlands at planting speeds; while others preferred to enter and exit headlands at a

slower turning speed, then accelerate to planting speed after turn negotiation. When planting

around a contour, the operator would typically decelerate for smaller radii contours and then accelerate once the contour was negotiated. In the events where the radius around the contour was large (typically > 100m), the operator would maintain a constant planting speed before, during, and after negotiating the contour.

Next, operator trends were observed when negotiating an in-field obstacle, such as a waterway, terrace or wet spot. The common trend found was for the operator to gradually decelerate, negotiate the obstacle, and then rapidly accelerate back to planting speeds. Lastly, several contour farming conditions were reviewed. Contour planting conditions could be across terraces, along field boundaries, or planting around environmental structures such as grassed waterways. The observed contour planting condition represented varying radii and speed differentials across the planter toolbar. Overall, observations from planting data indicated that typical planting speeds were in the range of 7.2 to 9.7 kph and acceleration/deceleration rates were from 1.4 kph/s to 2.1 kph/s. To quantify the performance of electric drive seed meters, planting speeds from 7.2 to 16.1 kph were selected for this study. The selected speeds represented both traditional planting speeds for straight-line and contour planting conditions; and higher planting speeds for increased productivity. The planter acceleration and deceleration of 2.1 kph/s was selected for headland operation; and of 1.4 kph/s to maneuver across an obstacle such as a wet spot in the field and to traverse across contours with a radius of <100 m.

Three simulation test scenarios (STS) in *.txt files were developed to conduct tests for the observed operator trends and planting scenarios. In STS1 the planter would 1) enter fields from headlands at 7.2 kph; 2) accelerate at 2.1 kph/s to planting speeds at 12.9 kph; 3) gradually decelerate at -1.4 kph/s to 7.2 kph to traverse the wet spot; 4) accelerate at 2.1 kph/s to attain a planting speed of 16.1 kph; 5) decelerate at -2.1 kph/s to 7.2 kph to enter the opposite headland;

and 6) repeat the scenario three times, Figure 3-1. STS1 is also represented in Table 3-1 broken

down into several key steps that occur during the simulation. The STS2 represented an operator

entering and exiting headlands without acceleration or deceleration. In STS2 the planter would

enter the headlands and exit the headlands at the desired planting speed, while maneuvering a

field obstacle in a fashion similar to STS1, Figure 3-2. STS2 is also represented in Table 3-2 as

a list of key steps. STS1 and STS2 also represented a point-row scenario, with instantaneous

seed meter engagement at headland entry and instantaneous disengagement at headland exit,

Figure 3-1 and 3-2.
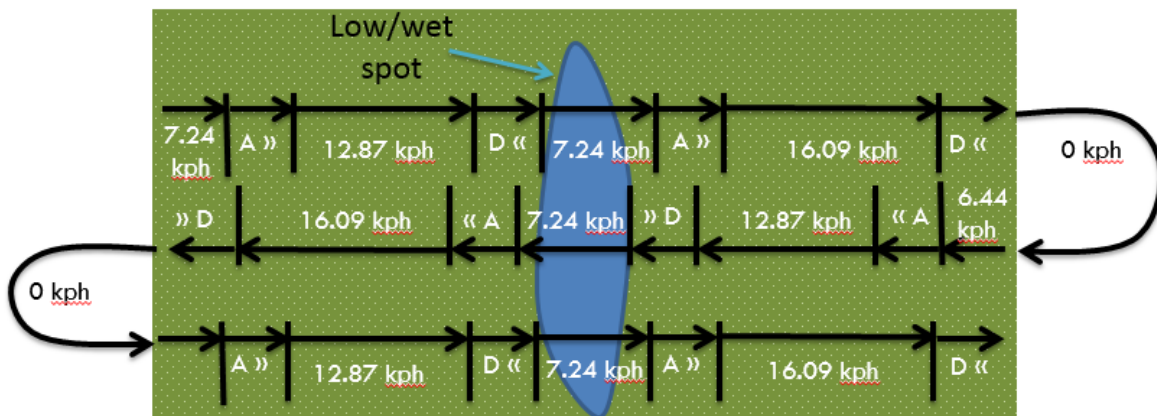
Figure 3-1 STS1, Spatial representation of simulated operator that decelerates/accelerates in/out of headlands when negotiating turns

Table 3-1 STS1, Steps of simulated operator that decelerates/accelerates in/out of headlands when negotiating turns

Simulation Step	Simulated Operation
Step 1 – Planter enters field	Planter enters the field at 7.24 kph, accelerates to 12.87k kph, and travels towards a wet spot at 12.87 kph, start of simulation
Step 2 – Obstacle negotiation	Planter decelerates to 7.24 kph, crosses a wet spot (obstacle), then accelerates back to planting speed at 16.09 kph
Step 3 – Headlands turn	Planter decelerates to 7.24 kph, enters headland, turns, and re-enters field in opposite direction at 6.44 kph, then accelerates to 12.87 kph
Step 4 – Obstacle negotiation	Planter decelerates to 7.24 kph, crosses a wet spot (obstacle), then accelerates back to planting speed at 16.09 kph
Step 5 – Headlands turn	Planter decelerates to 7.24 kph, enters headland, turns, and re-enters field in opposite direction at 6.44 kph, then accelerates to 12.87 kph
Step 6 – Obstacle negotiation	Planter decelerates to 7.24 kph, crosses a wet spot (obstacle), then accelerates back to planting speed at 16.09 kph
Step 7 – End of field	Planter decelerates to 7.24 kph, exits field through headlands, end of simulation
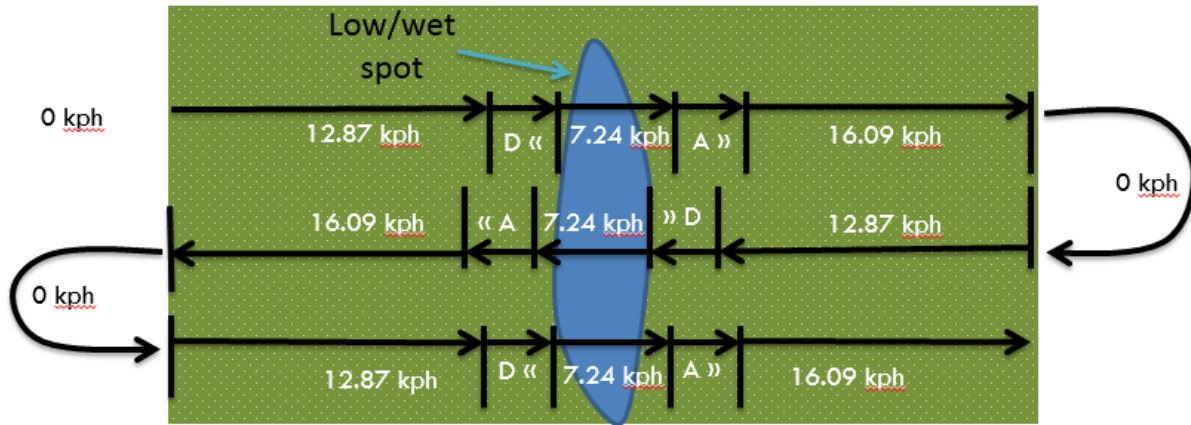
Figure 3-2 STS2, Spatial representation of simulated operator that enters/exits headlands at planting speeds when negotiating a turn

Table 3-2 STS2, Steps of simulated operator that enters/exits headlands at planting speeds when negotiating a turn

Simulation Step	Simulated Operation
Step 1 – Planter enters field	Planter enters the field and travels towards a wet spot at 12.87 kph, start of simulation
Step 2 – Obstacle negotiation	Planter decelerates to 7.24 kph, crosses a wet spot (obstacle), then accelerates back to planting speed at 16.09 kph
Step 3 – Headlands turn	Planter enters headland, turns, and re-enters field in opposite direction at 12.87 kph
Step 4 – Obstacle negotiation	Planter decelerates to 7.24 kph, crosses a wet spot (obstacle), then accelerates back to planting speed at 16.09 kph
Step 5 – Headlands turn	Planter enters headland, turns, and re-enters field in opposite direction at 12.87 kph
Step 6 – Obstacle negotiation	Planter decelerates to 7.24 kph, crosses a wet spot (obstacle), then accelerates back to planting speed at 16.09 kph
Step 7 – End of field	Planter exits field through headlands, end of simulation

For the final simulation, STS3, five curves with radii of 80, 100, 40, 150, and 20m were selected to evaluate the meters during contour farming. Planting speeds for straight runs and on contours of >100m were selected to be at 14.5kph. For contours with a radius of 50-100m the speed was set to 11kph. When negotiating smaller contours <50m but >20m the turning seed was set to 8kph. If the contour represented a very sharp turn with a radius <20m, the turning speed was set to 6kph. On all contours with a radius <100m, the acceleration and deceleration rate to and from straight-line speed was set at 2.1kph/s, Figure 3-3. The STS3 simulation steps are outlined in Table 3-3. To simulate the left and right ground radar speeds during a contour maneuver, the radar speeds were calculated using the desired turn radius and the planter toolbar width and location of the planter radars. The following equations were developed where outer radar speed is the radar located furthest from the center of the turn and the inner radar speed is the radar located closest to the center of the turn. (It should be noted that tractor speed and center radar speed were the same.)

$$Inner\ Radar\ Speed\ kph = (tractor\ speed\ kph) * \frac{turn\ radius}{turn\ radius\ +\ 9.1m}$$

$$Outer\ Radar\ Speed\ kph = (tractor\ speed\ kph) * \frac{turn\ radius\ +\ 18.3m}{turn\ radius + 9.1m}$$
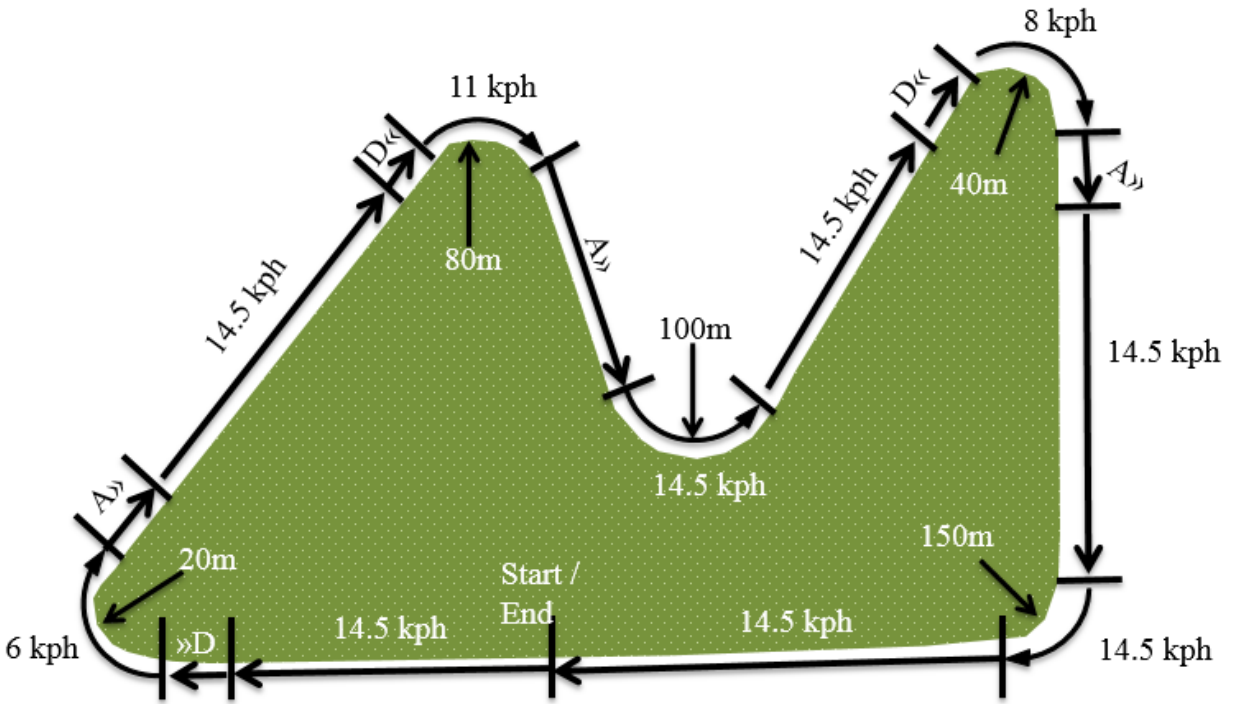
Figure 3-3 STS3, Spatial representation of simulated operator that negotiates contours while following the boundary of a field

Table 3-3 STS3, Steps of simulated operator that negotiates contours while following the boundary of a field

Simulation Step	Simulated Operation
Step 1 - Begin	Planter begins moving at 14.5 kph following field edge
Step 2 – 20m right turn	Planter decelerates to 6 kph and turns right on a 20m radius curve
Step 3 – Field edge	Planter accelerates out of turn to 14.5 kph and travels along the field edge
Step 4 – 80m right turn	Planter decelerates to 11 kph and turns right on an 80m radius curve
Step 5 – Field edge	Planter accelerates out of turn to 14.5 kph and travels along field edge
Step 6 – 100m left turn	Planter enters the 100m radius turn at 14.5 kph
Step 7- Field edge	Planter exits turn and continues on field edge at 14.5 kph
Step 8 – 40m right turn	Planter decelerates to 8 kph and turns right on a 40m radius curve
Step 9 – Field edge	Planter exits turn and accelerates to 14.5 kph across field edge
Step 10 – 150m right turn	Planter enters a 150m radius right turn at 14.5 kph
Step 11 – Field edge	Planter exits turn and follows field edge at 14.5 kph to test end

Simulation control and measurement system

A simulation text file was created for each STS. The simulation text file comprised of pre-determined speed signals representative of left, center, and right ground speed radars for straight runs, speed transitions at target acceleration and deceleration for headlands, obstacles, and contour farming operation. The speed signals from the simulation file were input into the Horsch controller in place of the planter's actual ground speed radars. A custom LabVIEW program (National Instruments, Austin, TX, USA) was developed to read the simulation text files at 10 Hz, parse the speed signals, and input the speeds into the Horsch controller.

A linear regression function, Figure 3-4, was fitted to speed, as displayed on the Horsch planter terminal, by inputting square wave frequencies generated using a signal generator (33500B, Agilent Technologies, Santa Clara, CA, USA) to mimic a ground speed radar's signal output. Since these tests were conducted with the planter in static state, the regression function was used to generate speed signals in the form of square wave frequencies for the Horsch ECU to mimic planting operation. A square waveform from 25 to 550 Hz to the Horsch ECU communicated the desired ground speed to the planter terminal. The ground signal parsed earlier was input into the regression function within the program to calculate the required square waveform frequency based on the STS simulation test file. The LabVIEW program generated the square waveform, representing the target ground speed, using a 5V TTL input/output module (9403, National Instruments, Austin, TX, USA) driving a step-up solid-state relay (70G-ODC5, Grayhill, La Grange, IL, USA) to convert the signal to 12V digital to drive the Horsch ECU's radar signal inputs.

To acquire seed meter motor speed data, rows 1, 4, 7, 10, 15, 18, 21, and 24 were outfitted with 3000 pulses per revolution thru-bore encoders (260-N-T-10-S-3000-Q-PP-1-S-FA-2-N, Encoder Product Company, Sagle, Idaho, USA) attached to the electronic seed meter's motor shaft via specially machined bushings, Figures 3-5 and 3-6. The seed distribution system was disabled for the rows with encoders to prevent seed interference with encoder operation. Encoder data was collected at 10Hz using a National Instruments CRio FPGA chassis and a C-Series module (9403, National Instruments, Austin, Texas, USA). A LabVIEW program recorded the encoder data and planter ground speed in real-time, at 10Hz, to a *.txt file for analysis.
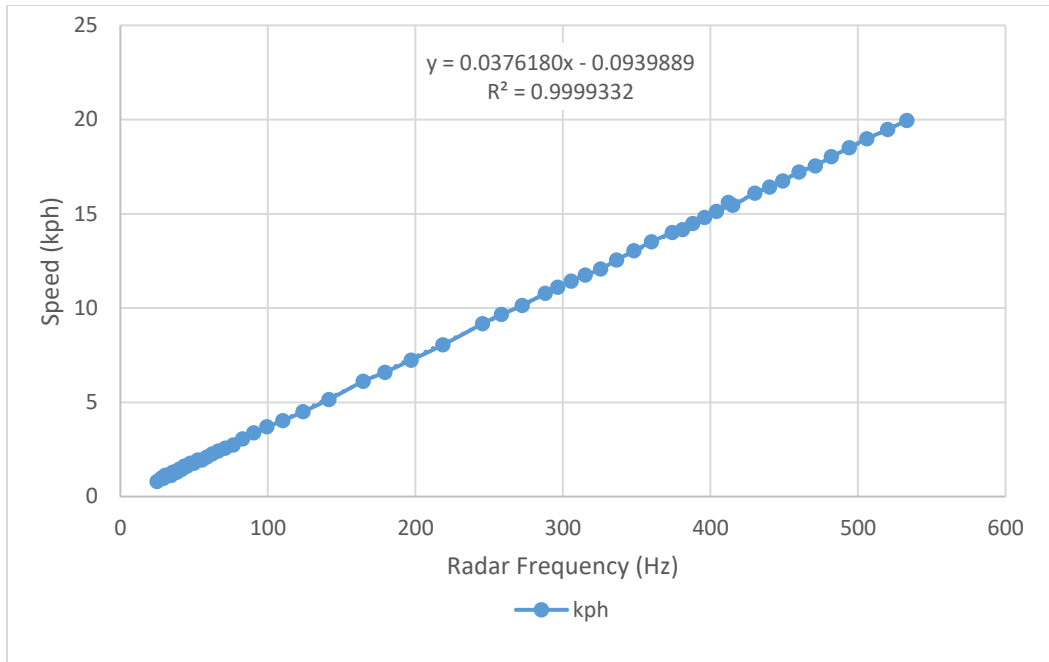
Figure 3-4 Relationship between ground speed and speed radar frequency output
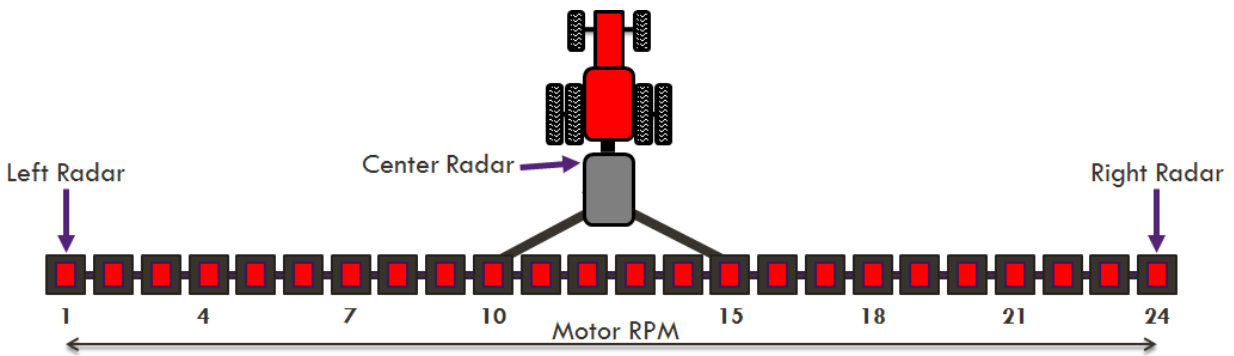
Figure 3-5 Locations of seed meter speed encoders and ground speed radars across the planter toolbar
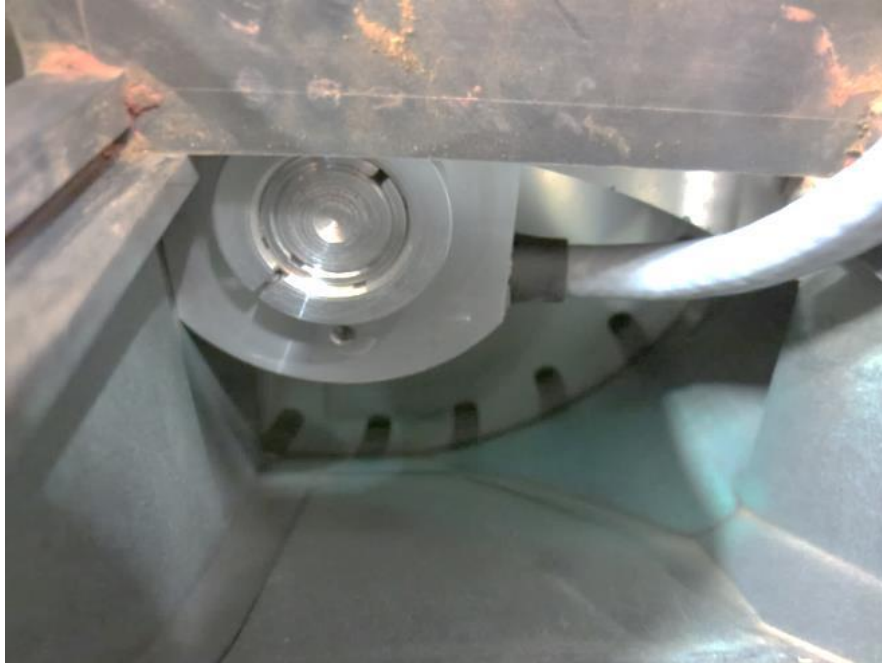
Figure 3-6 Seed meter speed encoder installed in meter housing on motor shaft

Experimental design and analysis

The three STSs were conducted at two seeding rates of 44,460 seeds/ha and 88,920 seeds/ha to simulate both a common high rate and a common low rate. STSs with two seeding rates and three replications were conducted in a random testing sequence to ensure repeatability and accuracy.

A linear function to relate electric seed meter speed to ground speed for both 44,460 seeds/ha and 88,920 seeds/ha was developed. The equations were developed for the planter setup utilizing 21 seeds/revolution seed plates, the two seeding rates, and a 0.8m row spacing. For 44,460 seeds/ha, motor rpm was equal to (13.9464)*(ground speed kph) and for 88,920 seeds/ha motor rpm was equal to (6.9770)*(ground speed kph).

Electric drive seed meter accuracy was determined by comparing actual meter rpm to the target

meter rpm at steady state and transient conditions. The differences in actual and target meter

speeds was used to calculate motor percent error for all thee STSs during both transient and

steady state operations. The difference in target meter speed and actual meter speed was also

used to calculate seed spacing variability and seeding rate variability.

The mean motor speed error for each row, and across different rows was, calculated for steady-

state conditions and motor response time was calculated for transient conditions. The meter

error was then related to seeding rate error. A Matlab (R2014a, MathWorks, Natick,

Massachusetts, USA) program was developed to quantify response time of each row motor for

the beginning and ending of each transient stage for all STS to measure response time for planter

accelerations and decelerations.   Using the same program, response time was determined for

point-row situations when meters where engaged from rest and when meters were disengaged

after entering headlands. The Matlab program, to measure response time, compared the target

motor speed to measured motor speed and calculated the time it took for the meter to achieve

target speed within ±3% of the target speed after a planter ground speed change was initiated.

Results and Discussion

After experiment completion, all test data were analyzed.

Steady state results

When operating in steady states, mean motor speed percent error varied from 0.1% to 1.5%.

When observing Figure 3-7, it can be seen that mean motor speed percent error decreases with

increased planter speed. The decrease in meter speed error at higher planting speeds was

believed to be related to the row unit's meter speed control mechanism, at higher speeds the

built-in meter speed encoders had a higher sampling rate resulting in a more accurate speed

average for the meter control unit to use within its control loop.
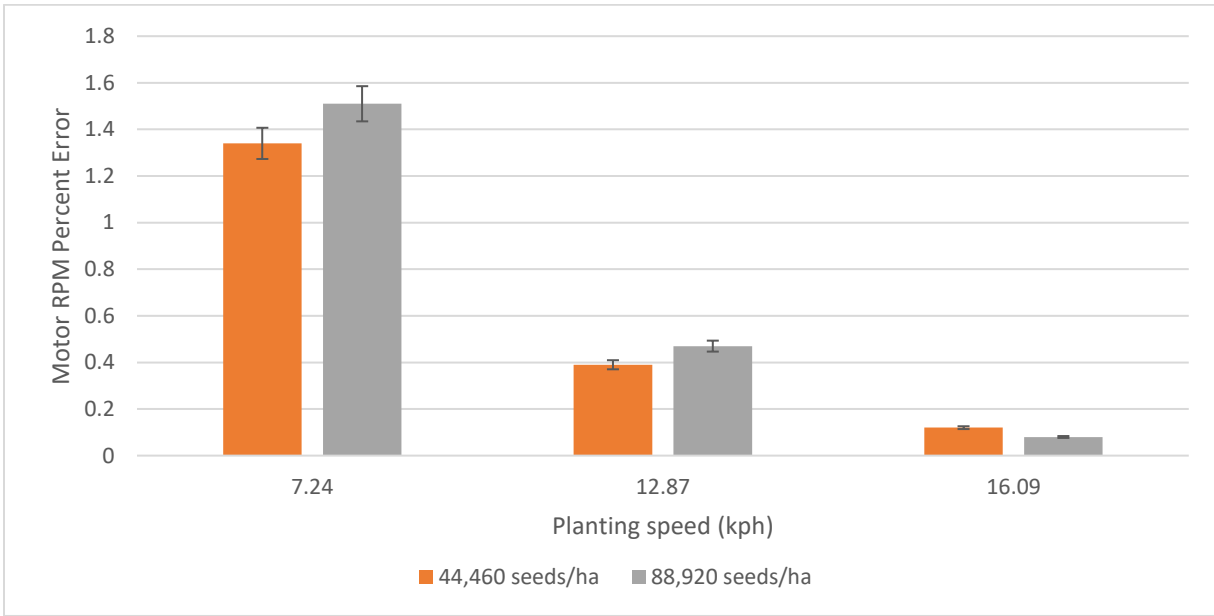
Figure 3-7 Mean percent error in meter RPM at constant speed

Row-to-row meter speed percent error standard deviation ranged from -0.03% to 0.19%. At the

highest observed meter speed percent error of 1.5%, the seed rate error, only based on the seed

motor speed error, was either ±1334 seeds/ha from target, which occurred at planting speeds

below 8.05 kph. At 16.09 kph, the average percent error was the lowest, averaging 0.2%, which

resulted in a seeding rate within ±54 seeds/ha of the target rate. A summary of seeding rate error

at the three steady-state speeds is provided in Table 3-4.

Table 3-4 Mean percent error in meter RPM and seed rate variability at constant speeds for STS1 and STS2

Speed (kph)	44,460 seeds/ha		88,920 seeds/ha	
	% Error	Seed Rate Variability (seeds/ha)	% Error	Seed Rate Variability (seeds/ha)
7.24	1.35	± 600	1.5	± 1334
12.87	.4	± 178	.48	± 427
16.09	.1	± 44	.06	± 54

After calculating the overall mean percent error, the mean row to row variability was calculated. It was found that the highest row to row variability at any speed was 1.5% which equates to the row units always being within plus or minus 1334 seeds/ha of each other at all times. Tables 3-5 and 3-6 list individual meter error at both 18,000 seeds/acre and 36,000 seeds/acre. In Tables 3-5 and 3-6, row 18 is omitted at 16.09 kph because of a row unit failure during these tests.

Table 3-5 Average percent row-to-row motor speed error for STS1 and STS2 (44,460 seeds/ha)

Speed (kph)	Percent error in RPM								Average % Error	Standard Deviation
	Row 1	Row 4	Row 7	Row 10	Row 15	Row 18	Row 21	Row 24		
7.24	1.33	1.39	1.37	1.38	1.35	1.19	1.33	1.35	1.34	0.06
12.87	0.38	0.43	0.51	0.44	0.39	0.17	0.38	0.44	0.39	0.10
16.09	0.18	0.11	0.12	0.11	0.11	-	0.07	0.13	0.12	0.03

Table 3-6 Average percent row-to-row motor speed error for STS1 and STS2 (88,920 seeds/ha)

Speed (kph)	Percent error in RPM								Average % Error	Standard Deviation
	Row 1	Row 4	Row 7	Row 10	Row 15	Row 18	Row 21	Row 24		
7.24	1.52	1.60	1.53	1.59	1.48	1.32	1.57	1.45	1.51	0.09
12.87	0.53	0.47	0.58	0.59	0.56	0.02	0.48	0.55	0.47	0.19
16.09	0.11	0.09	0.09	0.09	0.08	-	0.05	0.03	0.08	0.03

Transient state results

The mean response times, for transient states, are shown in Table 3-7. On average, the row motor response time was within 0.15 seconds during speed changes in STS1 and STS2. During the transient states (accelerations and decelerations) of STS1 and STS2, the meters maintained their speed to within 0.65rpm of target speed and 1.41rpm of target speed for 44,460 seeds/ha and 88,920 seeds/ha seeding rates respectively, Table 3-8. The measured meter speed differences for both acceleration and deceleration lead to a seeding rate error of ±1030 seeds/ha and a seed spacing error of ±0.68 cm at a seeding rate of 44,460 seeds/ha as well as a seeding rate error of ±2214 seeds/ha and a seed spacing error of ±0.36 cm at 88,920 seeds/ha seeding rate. During the transient states at both seeding rates the meter speed error was higher during accelerations than decelerations, Table 3-8.

Table 3-7 Mean meter response time during STS1 and STS2 transient states

Seeding Rate (Seeds/ha)	Speed Transition (kph)	Time (seconds)
44,460	7 – 16.1	0.1
	12.9 – 7.2	0.1
88,920	7.2 – 16.1	0.3
	12.9 – 7.2	0.3

Table 3-8 Mean meter speed, seed spacing, and seeding rate difference during STS1 and STS2 transient states

Seeding Rate (Seeds/ha)	Meter speed, seed spacing, and seed rate difference during acceleration	Meter speed, seed spacing, seed rate difference during deceleration	Overall meter speed, seed spacing, and seeding rate difference for acceleration and deceleration
44,460	+0.60 rpm	-0.70 rpm	±0.65 rpm
	+0.54 cm	-0.82 cm	±0.68 cm
	-792 seeds/ha	+1269 seeds/ha	±1030 seeds/ha
88,920	+1.37 rpm	-1.44 rpm	±1.41 rpm
	+0.32 cm	-0.41 cm	±0.36 cm
	-1880 seeds/ha	+2547 seeds/ha	±2214 seeds/ha

In Figure 3-8, an example of an acceleration from 7.2 to 16.1 kph in three seconds at a seeding rate of 88,920 seeds/ha is presented. The acceleration led to the planter operating at slight under-seeding conditions. As the planter accelerated, there was a 0.2 second delay to respond to the speed increase. During planter acceleration, the actual motor speeds were 1.37 rpm lower than the target speeds. The lower than target motor speed could lead to the planter operating at slight under-seeding conditions during accelerating scenarios. The current seed rate during this

54

acceleration was at or within -1880 seeds/ha of the target seed rate of 88,920 seeds/ha. This

creates a max spacing error during accelerations of +0.32 cm of target seed spacing.

The response of the motors during deceleration was similar to what was observed during

accelerating scenarios. An example of a deceleration is shown in Figure 3-9 where speed was

decreased from 12.87 to 7.24 kph in four seconds at a seeding rate of 88,920 seeds/ha. The

deceleration was representative of an operator slowing for an obstacle or slowing to enter a

field's headlands. The motors exhibited a 0.3 second delay when responding to the ground speed

change. The actual motor speed was always 1.44 rpm higher than the target speed during

deceleration. The deceleration lead to slight over seeding conditions during the transient stage.

The seeding rate was always at or within +2547 seeds/ha of the target rate of 88,920 seeds/ha.

This resulted in the seed spacing to be at or within -0.41 cm of the target seed spacing.
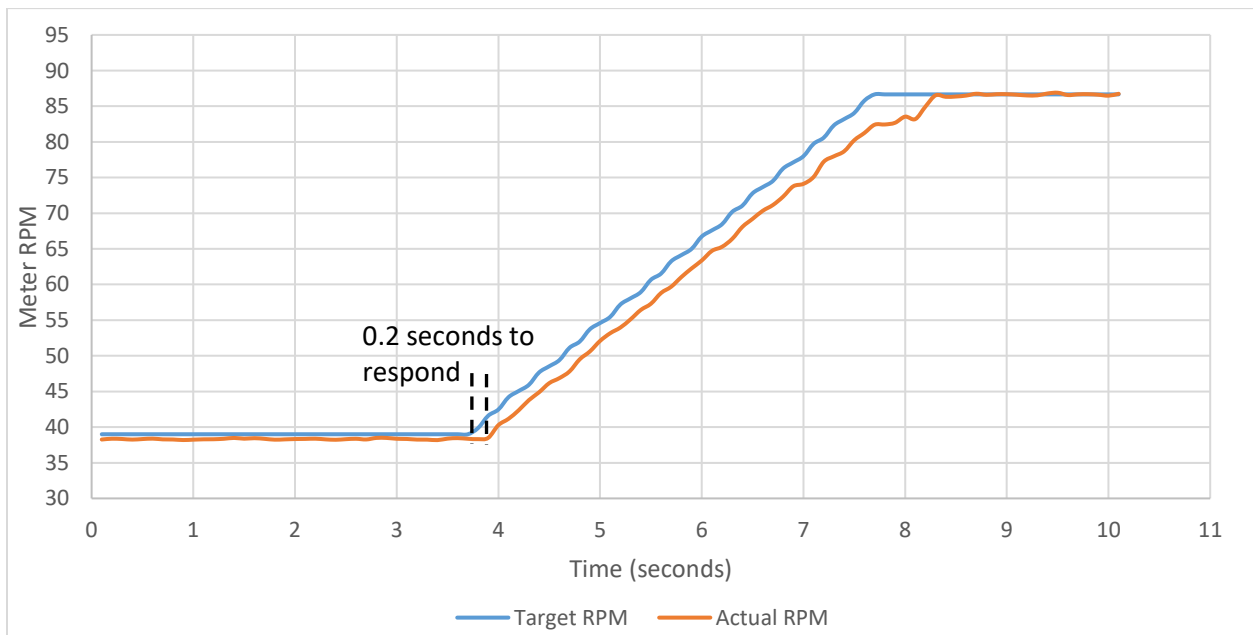
Figure 3-8 Acceleration from 7.24 to 16.09 kph, at 88,920 seeds/ha
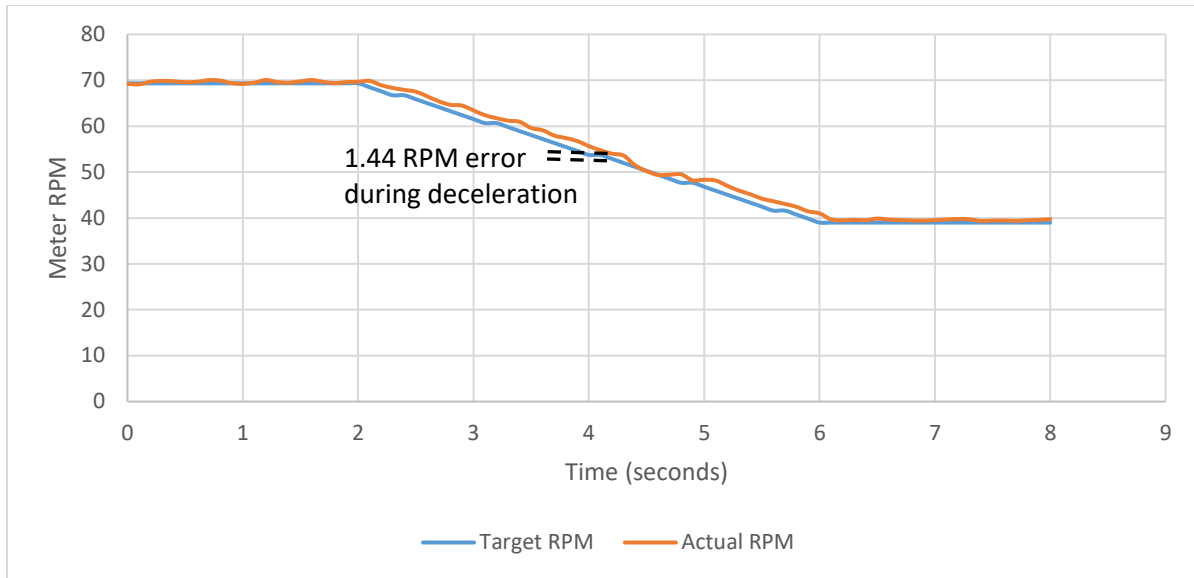
Figure 3-9 Deceleration from 12.87 to 7.24 kph, at 88,920 seeds/ha

Point-Row simulation results

Response time of the row meters during STS2 indicated that 0.3 seconds would pass, 1.2m were travelled, before the meter began to respond to the instant speed increase, Figure 3-10. This delay resulted in five seeds, at a seeding rate of 44,460 seeds/ha, being affected and not placed due to the meter's response time. Similarly, the response time of an instantaneous speed decrease exhibited that 0.3 seconds passed, or 1.2m were travelled, before the meter began to respond to the speed decrease, Figure 3-11. This results in four seeds, at a seeding rate of 44,460 seeds/ha, being overplanted due to the meter's response time. Therefore, a look ahead time of 0.5 seconds might be programmed in the Horsch ECU for timely actuation of row motors to accurately maintain the seeding rates when performing point-row operations.
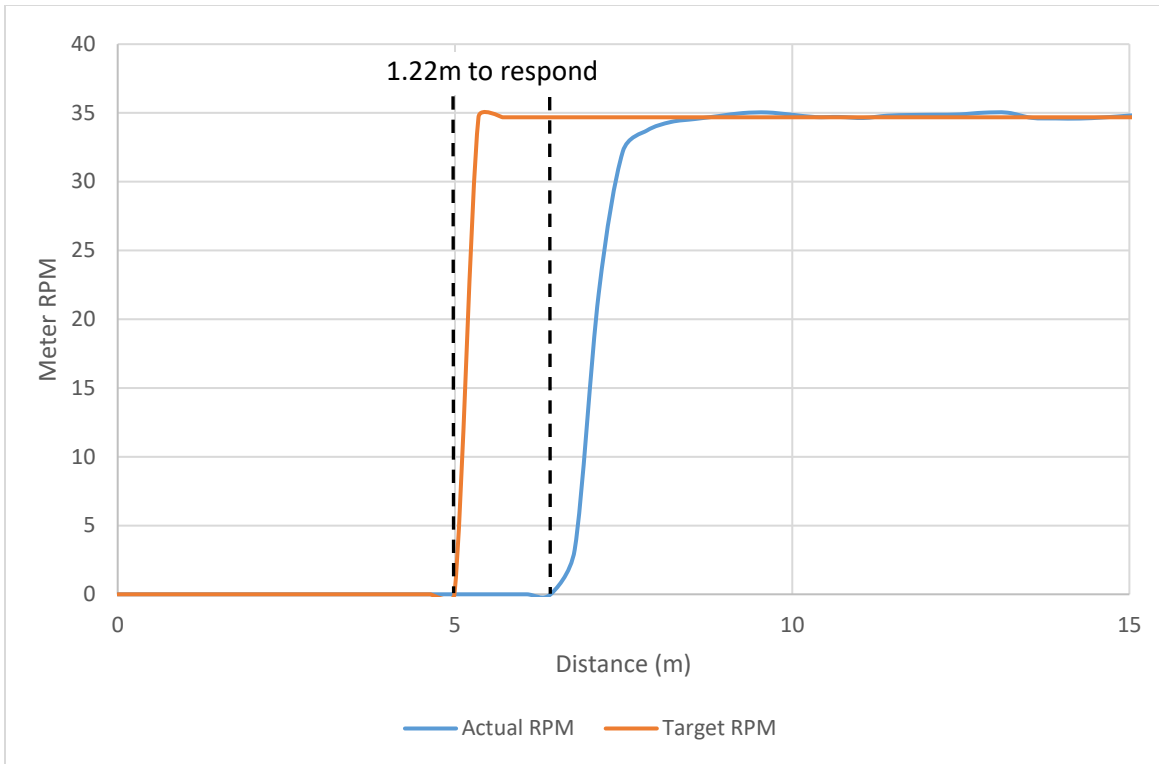
Figure 3-10 Point-Row simulation, 0 to 12.87 kph, at 44,460 seeds/ha
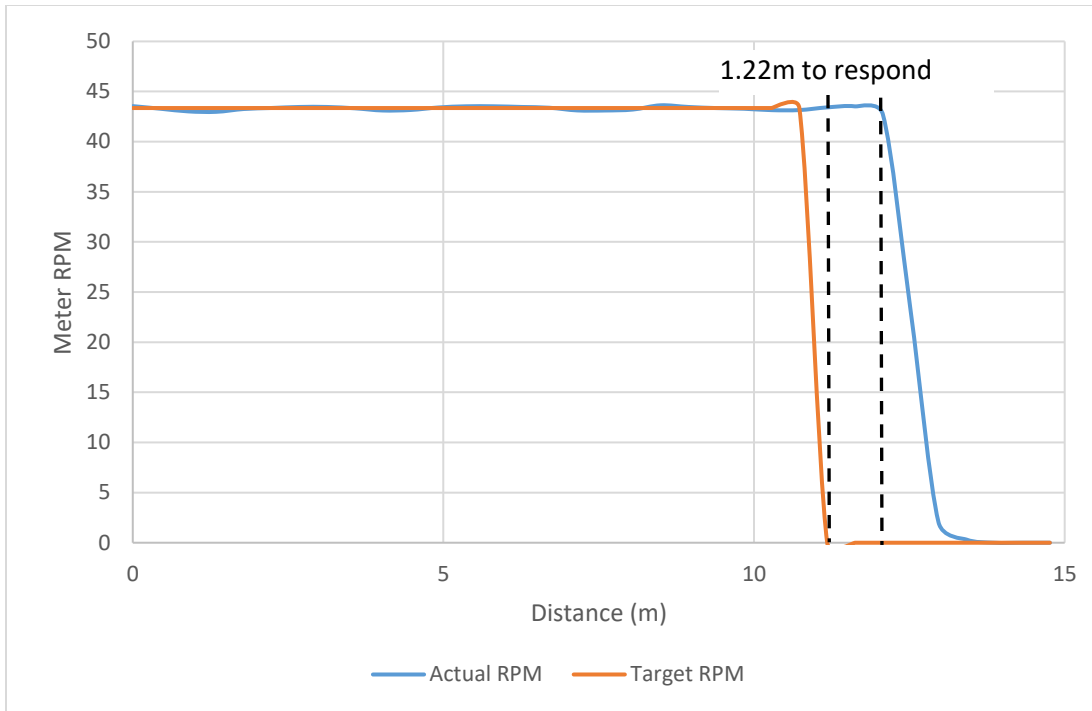
Figure 3-11 Point-Row simulation, 16.09 to 0 kph, at 44,460 seeds/ha

Contour farming results

When a simulated contour was encountered, the planter's ECU gradually varied individual meter speed to match the target meter speed based on the tractor's turn radius. The innermost row unit of a turn experienced the slowest ground speed whereas the outermost row unit experienced the largest ground speed. This operation is expressed in Figure 3-12 showing the planter in a right-turn contour maneuver at 8 kph and then exiting and accelerating back to straight-line planting speed at 14.5 kph. This contour maneuver produced a meter speed difference of 17 rpm from row unit one to row unit 24 across the planter toolbar requiring each row to operate at a different speed to maintain proper seed spacing. When the planter experienced the start or end of a contour maneuver, 0.3 seconds were taken before the planter responded and the motors began to

adjust speed, this can lead to four seeds being over or under placed in each row during the time of response.
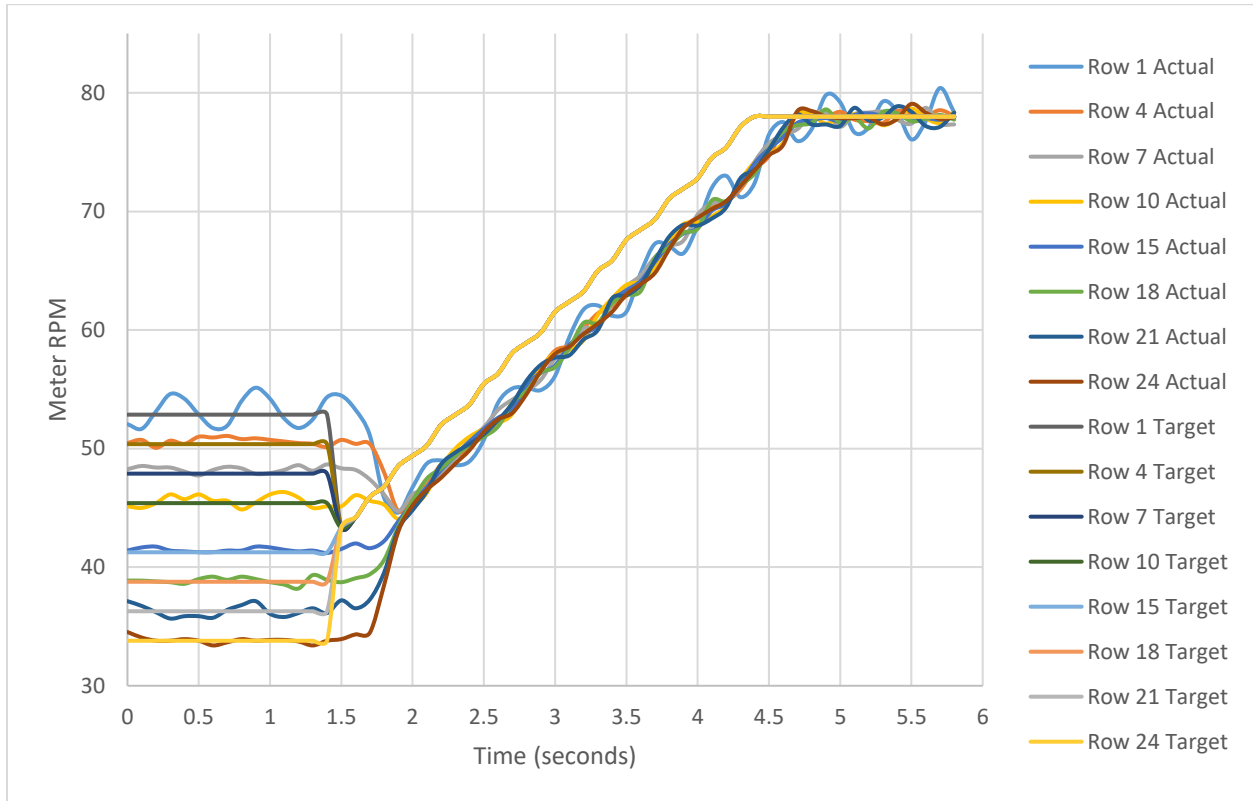
Figure 3-12 Planter exiting a right-turn contour negotiation at 8 kph and a radius of 40m, then returning to straight-line planting speed at 14.5 kph during STS3, (88,920 seeds/ha)

During contour operations of the planter, mean motor rpm percent error was maintained below 1.4% for all motors during all simulated contours. An error of 1.4% results in the meters always being within 1334 seeds/ha of the target rate during contour operation. The mean motor speed error for each row during each simulated contour is listed in Tables 3-9 and 3-10. These tables also list the overall average error for each contour that was simulated. During contour negations

with a large speed offset across the planter toolbar, meter speed error could vary as much as

0.65% across the planter's row units.

Table 3-9 Average percent error in meter RPM (44,460 seeds/ha)

Turn Radius (m)	Percent error in RPM								Average % error across the planter	Standard Deviation
	Row 1	Row 4	Row 7	Row 10	Row 15	Row 18	Row 21	Row 24		
20	0.47	0.43	0.64	0.52	0.62	0.55	0.81	1.22	0.66	0.26
40	0.47	0.52	0.56	0.27	0.33	0.32	0.23	0.09	0.35	0.16
80	0.12	0.10	0.01	0.07	0.00	1.07	0.02	0.06	0.18	0.06
100	0.27	0.35	0.42	0.47	0.50	0.92	0.62	0.72	0.53	0.21
150	0.09	0.11	0.20	0.18	0.11	0.49	0.14	0.13	0.18	0.13

Table 3-10 Average percent error in meter RPM (88,920 seeds/ha)

Turn Radius (m)	Percent error in RPM								Average % error across the planter	Standard Deviation
	Row 1	Row 4	Row 7	Row 10	Row 15	Row 18	Row 21	Row 24		
20	0.54	0.53	0.63	0.65	0.86	0.90	1.02	1.38	0.81	0.29
40	0.66	0.63	0.64	0.45	0.47	0.26	0.20	0.23	0.44	0.19
80	0.22	0.18	0.18	0.13	0.12	0.05	0.04	0.01	0.12	0.08
100	0.08	0.17	0.35	0.28	0.40	0.69	0.57	0.61	0.39	0.22
150	0.04	0.02	0.07	0.03	0.03	-	0.04	0.03	0.04	0.02

Conclusion

An electronic drive seed meter was evaluated for its capability to maintain target operating speed, its ability to transition from one speed to another during acceleration and deceleration in straight-line and contour field scenarios, and its ability to engage and disengage during point-row scenarios. The results of these tests showed that the electronic drive could maintain target speed to within ±1,334 seeds/ha of the target seeding rate for all steady state tests. During straight-line acceleration and deceleration of the planter, a maximum time of 0.3 seconds was needed to respond to a speed change. This response time resulted in the planter being within ±1,030 seeds/ha and ±2,214 seeds/ha of the 44,460 seeds/ha and 88,920 seeds/ha target seeding rates respectively during all speed transitions. During contour farming scenarios, the electronic drive seed meters were always at or lower than 1.38% meter speed error throughout the contour. This results in the meters always maintaining target seeding rate within ±1,334 seeds/ha of the target seeding rate during a contour maneuver.

The tests also showed that the seed meters were able to maintain a lower meter speed error when operated at higher planting speeds. This is theorized to be caused by the electronic meter's control loop system. The meter speed control loop would have a larger sampling rate at higher speeds allowing the meters to produce a more accurately controlled speed when operated at high planting speeds. When performing point-row operations, the response time of the meters was always less than 0.34 seconds. This response time correlated to a maximum of five seeds being over planted or under planted at the target seeding rates. This is useful information for producers because if a look-ahead time of 0.5 seconds, for example, is used in the Horsch controller, the under and overplanting at the headlands could be nearly eliminated.

61

Based on this study, the performance of the electric drive utilized on the studied seed metering systems is appropriate for use at higher planting speeds and/or for contour farming. The meters increased in accuracy as speed increased and percent error was always less than 1.5%, resulting in the actual seeding rate of the meters being within ±1334 seeds/ha of the target rate under all steady-state conditions. With the high seeding accuracy at high speeds, the end users can be assured that the proper seeding rate is being applied. The accuracy of these meters was not affected by a high or low seeding rate as much as the operating speed. Although the electronic drive component of the studied seed meter is acceptable for high planting speeds, the singulation abilities of the meter still need to be evaluated at high speeds to ensure proper seed singulation throughout the entire metering system during high speed operation.

Chapter 4 - Conclusion

In summary, a test stand was designed, constructed, and evaluated for use as a means to quantify the performance of production row crop planter automatic downforce systems. The test stand consisted of a horizontal platform that could be raised and lowered to simulate soil terrain changes as well as a mechanism to change the applied load to the planter row unit's opening discs, thereby simulating soil texture changes. The test stand was then used to do evaluations of an automatic hydraulic downforce system. Field data was used to create simulation files that were then parsed through the test stand's controller to replicate the field data. Several situations were evaluated which included planter speed changes, soil texture changes, and an extreme condition with a hard/rocky clay soil. The results were used to determine the time that the planter's downforce system maintained gauge wheel loading within three target ranges of the set gauge wheel load as well as the downforce system's response to rapid disc load changes.

Also conducted was an evaluation of a production row crop planter electronic drive singulation seed meter. The electronic drive seed meter was evaluated to quantify its performance during simulated in-field scenarios that occur in a typical Kansas field. The seed meter was evaluated through the use of a 24 row production planter with encoders mounted on the seed meter shafts to gather the actual speed of the seed meter, this speed was then compared to the target seed meter speed. The scenarios simulated were accelerations, decelerations, point-rows, and contours. The seed meter's performance was then used to determine effects on seed rate stability.

Summary of Findings

In Chapters two and three, two separate components of a production planter were evaluated. In

Chapter two a planter downforce test stand was constructed and used to evaluate a production

planter's automatic hydraulic downforce system during simulated field conditions. In Chapter

three the electronically driven seed meters of the same planter were evaluated for their

performance during simulated field operations. The following is a summary of results obtained

from the testing completed in each Chapter.

Automatic downforce system control during planting speed changes

After the downforce test stand was designed, constructed, and evaluated, it was used to quantify

the response of a production row crop planter row unit equipped with an automatic downforce

control system. The first simulated field scenarios emulated the planter row unit traversing a

field at three different planting speeds of 7.2 kph, 9.7 kph, and 12 kph with the same soil type.

From these tests it was found that the speed the planter traveled at affected the dynamic disc

loading. At a higher speed, the undulations of the disc loading seemed to be lower than when at

a slower planting speed. This is theorized to be due to the effects of the planter's momentum at a

higher speed allowing the opening discs to penetrate the soil easier with less spikes in load.

Although there was a change in the disc load variations with speed, the planter's automatic

downforce controller was able to maintain the target gauge wheel load to within ±223 N of target

gauge wheel load at least 99% of the time for all three speed tests. When looking at how well

the controller maintained a narrower target gauge wheel load range of ±89 N, a change in the

percent time within range varied with speed. At a slower speed of 7.2 kph, the controller

maintained the target range of ±89 N 72% of the time. When traversing at 9.7 kph the controller

maintained gauge wheel load within ±89 N of target for 62% of the time. But, when operated at

a higher speed of 12 kph, the planter maintained gauge wheel load within ±89 N of target 89% of

the test.

Automatic downforce system control during a soil texture change

When the planter was simulated to have passed through a soil texture change, the average disc

loading was either increased or decreased. This demanded the automatic downforce system

adjust its output load to maintain the target gauge wheel load. These adjustments that must be

made by the controller are larger than what is seen during the speed tests where the average disc

loading is constant. Although this created a larger demand for adjustment, the controller was

able to maintain the gauge wheel load to within ±223 N of target gauge wheel load for 96% and

100% of the time for each test.

Automatic downforce system control during extreme field conditions

The final downforce simulation conducted simulated the planter row unit crossing a field

headland with a hard/rocky clay soil. This situation caused higher variations in disc load than

the speed or texture change tests. Throughout the hard/rocky clay test, the required disc load

average also varied more than the other tests. This required fast reaction times for the controller

to properly maintain gauge wheel load within a target range. The results showed that the

controller could maintain the gauge wheel load within ±223 N of the target load for 94% of the

test. When evaluating the planter's control capabilities under a narrower range of ±89 N, the

controller maintained the gauge wheel load within range for 60% of the test.

Automatic downforce system response to disc load changes

To begin to understand the response time of the automatic downforce controller, three disc load change events were selected. These events represented a typical, smaller load change of 186 N, a medium load change of 412 N, and a large load change of 687 N. The events occurred over a time span of 1, 3.1, and 2.2 seconds respectively. For these events, the time that the planter was out of a ±223 N range from the target gauge wheel load was calculated. For the first two load change events of 186 N and 412 N, the gauge wheel load was always within ±223 N of the target gauge wheel load. For the final test of a large disc load change of 687 N, the gauge wheel load was outside of the target ±223 N range for 1.3 seconds.

Electronic singulation seed meter steady state performance

To test the steady-state electronic meter speed control the planter was sent several simulated ground speeds. These speeds represented the planter traveling through a field at a constant speed. Three speeds of 7.24 kph, 12.87 kph, and 16.09 kph were chosen because these represent a traditional, slower planting speed (7.24 kph) and two high planting speeds to compare meter performance at both ends of a typical planting speed range. It was found that at a slower speed of 7.24 kph, the planter seed meters had a higher motor rpm error than when operated at higher planting speeds. At 7.24 kph, 12.87 kph, and 16.09 kph the meter speed errors were 1.35-1.5%, 0.4-0.48%, and 0.1-0.06% respectively, Figure 3-7. Also analyzed was the mean row-to-row meter speed variability. The highest meter speed error recorded was 1.51%, Figure 3-7. Throughout all steady-state operation, the overall average meter speed variability was 0.65% with a standard deviation range of -0.03% to 0.19%.

Next, the meter speed error was associated with seeding rate error for easy relation to the set plating rate. At the maximum average seed meter speed error of 1.5%, at a seeding rate of 88,920 seeds/ha and 7.24 kph, the seed rate variability was ±1334 seeds/ha. At a high planting speed of 16.09 kph, the highest seeding rate variability was at 88,920 seeds/ha with a seeding rate error of ±54 seeds/ha, Table 3-4. The reduction in meter accuracy at lower speeds is attributed to the motor controller's sampling system which would have less pulses per amount of time received at a slower speed, thus lowering the controller's speed resolution.

Electronic singulation seed meter transient state results

For each speed transition tested, a Matlab program was used to calculate the average response time of the seed meters. When the meters experienced a speed transition from 7.24 kph – 16.09 kph, the controller maintained an average response time of 0.2 seconds for both tested seeding rates. When the planter experienced a deceleration from 12.87 kph – 7.24 kph, the planter's controller maintained an average response time of 0.1 seconds. This resulted in a maximum seeding rate error of -1880 seeds/ha of target when experiencing an acceleration at 88,920 seeds/ha and a maximum seeding rate error of +1269 seeds/ha during a deceleration at a target rate of 44,460 seeds/ha, Table 3-8. The rate error was maintained throughout the entire speed transition but was corrected after the acceleration or deceleration ended and the meters went back into steady state operation.

Electronic singulation seed meter point-row simulation results

Point-row conditions were simulated by instantaneously changing the simulated panting speed instantaneously to 0 kph or by changing the planting speed from 0 kph to a planting speed instantaneously. To quantify the meter's response time to the simulated point-row scenarios, the

previously mentioned Matlab program was utilized. The program found that, during a meter speed transition from 0 to planting speed, the response of the meters was 0.34 seconds. During an instantaneous speed stop, the meters took 0.27 seconds to respond. This resulted in a maximum of 4 seeds being over placed when stopping the planter, and 5 seeds not being placed when starting. Using this information, producers or machine operators could set a look-ahead time of 0.4 - 0.5 seconds, for example, to nearly eliminate over and under planting at headlands in point-row situations.

Electronic singulation seed meter contour simulation results

To simulate the planter turning to follow a contour in a field, the outside radars on the planter received speeds that represented the speed differential that the planter would experience across the toolbar. Five turning radii of 20 m, 40 m, 80 m, 100 m, and 150 m were simulated. During a contour operation, the planter must vary each meter speed individually and maintain a different speed at each seed meter. During all contour simulations the planter maintained mean motor speed error below 1.38%, Tables 3-9 and 3-10. This results in the planter always maintain the planting rate within 1334 seeds/ha of the target rate for all simulated contours.

Implications

The knowledge gained from both the downforce and electronically driven seed meter testing can not only be used for further evaluation of planting systems, but can also be used by producers who must choose between the available production planting technologies. Knowing that the tested hydraulic downforce system can maintain target gauge wheel loading within ±223 N of the set gauge wheel load, for over 93% of all tests, can be used as a deciding point for producers

looking at a traditional system or an automatically controlled system. If the producer is operating on fields with little soil texture variation then the added cost of an automatically controlled downforce system may not be feasible. Whereas if the produce has fields of varying textures, they may seriously consider the added cost of the systems to ensure that their set seeding depths are maintained more accurately to increase crop yield potential.

When considering seed meter drive technologies, a producer must consider their field conditions that the planter will operate under. With individual electronically driven seed meters, many precision planting features can be added without any hardware changes. This is evident in many newer planting technologies that include these features because the hardware natively supports it. When comparing seed meter drive technologies a producer can use the included research to make decisions on the accuracies required for them. If a producer does not encounter contours in their fields, or many point-row situations, a traditionally ground-driven planter may be more suited to their needs.

Now that the accuracies of an electronically driven seed meter have been explored, other areas of the seed metering and delivery system can be evaluated for their individual errors. Once all errors of the complete seed metering and delivery system are evaluated, individual components can be targeted for improvement.

Research limitations

Although a downforce test stand was constructed and evaluated for the simulation of both terrain and texture changes, no field data was available with terrain change data. Therefore, all simulations were conducted at a constant platform height. To further this research, data should be collected with both terrain and texture changes recorded. This would allow for a more real-

life evaluation of automatic downforce systems to occur. Another aspect of the downforce test stand is the speed of the pneumatic systems. While the pneumatic systems can accurately reproduce the average changes in disc loading that occurs in field data, it cannot replicate the shock loadings seen by the row unit traversing across the ground. To remedy this, and test the effects of shock loading, the test stand could be retrofitted or re-designed using hydraulics to increase the speed at which load changes can be made. Pneumatics were originally chosen for the test stand due to the much higher cost of a full hydraulic system.

The results obtained from the testing of the electronic drive singulation seed meters represents the ability for the meter's drive system itself to maintain target speed, and therefore target seeding rate. The seed rates errors found from meter performance testing only represent the seed meter itself, it does not represent the singulation abilities of the seed plate and vacuum system or the abilities of the delivery system and furrow placement system that are also responsible for accurately maintaining seed spacing.

Future Research

To further evaluate automatic downforce systems, field data needs to be collected which includes disc load variations as well as terrain changes. This could then be used to re-evaluate the hydraulic downforce system that was tested. The test results could then be used to adjust the hydraulic system's control loop parameters for better operation. After the control loops are changed, the system could be re-tested and the effects of the changes evaluated. Eventually this method would result in a more accurately tuned downforce system. Also, a parameter could be added to the control loop for speed compensation that adjusts the control's "aggressiveness" with

speed to more accurately maintain gauge wheel load and seeding depth throughout planting speed changes.

Although the ability to measure and record the planter ECU's PWM output was incorporated into the downforce test stand, this was not used for evaluation of the automatic downforce system. The PWM data could be compared to the row unit's hydraulic pressure and the response of the hydraulic system itself could be gained. This would further break down the automatic downforce system's overall response and error and allow for improvements to be targeted at a specific system with the highest amount of error or the lowest response time.

Future research that would be particularly useful to producers would be a study of the cost effectiveness of each system and the payoff time required for each system. This would be of the most benefit to producers who are making choices between several production planters with varying levels of technology.

References

American Society of Agricultural and Biological Engineers, (2014). ASABE S506: Terminology and Definitions for Planters, Drills and Seeders, St. Joseph, MI: Power and Machinery.

Automatic Section Control, Advanced Planting Technology Offers Benefits to Corn, Soybean Farmers. (2013, August 02). Corn and Soybean Digest.

E. T. Weatherly, C. G. Bowers Jr. (1997). Automatic depth control of a seed planter based on soil drying front sensing. Transactions of the ASAE, 40(2), 295.

Grisso, R., M. Alley, D. Holshouser, and W. Thomason. (2009). Precision farming tools: Soil electrical conductivity. Virginia Cooperative Extension. Retrieved from https://pubs.ext.vt.edu/442/442-508/442-508_pdf.pdf

H. M. Hanna, B. L. Steward, L. Aldinger. (2010). Soil loading effects of planter depth-gauge wheels on early corn growth. Applied Engineering in Agriculture, 26(4), 551.

Koller, A., Wan, Y., Miller, E., Weckler, P., & Taylor, R. (2014). Test Method for Precision Seed Singulation Systems. Transactions of the ASABE, 1283-1290. doi:10.13031/trans.57.10466

Liu, W., Tollenaar, M., Stewart, G., & Deen, W. (2004). Impact of Planter Type, Planting Speed, and Tillage on Stand Uniformity and Yield of Corn. Agronomy Journal,96(6), 1668. doi:10.2134/agronj2004.1668

Liu, W., Tollenaar, M., Stewart, G., & Deen, W. (2004). Response of Corn Grain Yield to Spatial and Temporal Variability in Emergence. Crop Science,44(3), 847. doi:10.2135/cropsci2004.8470

Miller, E. A., Rascon, J., Koller, A., Porter, W. M., Taylor, R. K., Raun, W. R., & Kochenower, R.

(2012). Evaluation of Corn Seed Vacuum Metering Systems. 2012 Dallas, Texas, July 29 - August 1, 2012. doi:10.13031/2013.42140

Morrison, J. E., Jr. (1988). Hydraulic Downpressure System Performance for Conservation Planting Machines. Transactions of the ASAE,31(1), 0019-0023. doi:10.13031/2013.30658

Morrison, J. E., Jr. (1988). Interactive Planter Depth Control and Pneumatic Downpressure System. Transactions of the ASAE,31(1), 0014-0018. doi:10.13031/2013.30657

Morrison, J. E., Jr., Hendrick, J. G., III, & Schafer, R. L. (1996). Soil Forces on Coulter and Disc-opener Combinations. Transactions of the ASAE,39(2), 369-376. doi:10.13031/2013.27511

Nielsen, R. L. (2004, May 2). Requirements for Uniform Germination and Emergence of Corn. Retrieved June 13, 2017, from http://www.agry.purdue.edu/ext/corn/news/timeless/GermEmergReq.html

Nielsen, R. L. (2005). Effect of Plant Spacing Variability on Corn Grain Yield. Retrieved June 12, 2017, from http://www.agry.purdue.edu/ext/corn/research/psv/Update2004.html

Sharda, A., Fulton, J., Badua, S., Griffin, T., Ciampitti, I., & Haag, L. (2017). Planter downforce technology for uniform seed depth. K-State Extension. Retrieved from http://www.bookstore.ksre.ksu.edu/pubs/MF3331.pdf

Sharda, A., S. Badua, D. Flippo, T. W. Griffin, and I. Ciampitti. (2016). Real-time gauge wheel load variability on planter with downforce control during field operation. In proceeding of the 13th International Conference on Precision Agriculture, St. Louis, Missouri, U.S., July 31st to 2nd, 2016.

Staggenborg, S. A., Taylor, R. K., & Maddux, L. D. (2004). Effect Of Planter Speed And Seed

Firmers On Corn Stand Establishment. Applied Engineering in Agriculture,20(5), 573-580.

doi:10.13031/2013.17457

Velandia, M., Buschermohle, M., Larson, J. A., Thompson, N. M., & Jernigan, B. M. (2013). The

economics of automatic section control technology for planters: A case study of middle and west

Tennessee farms. Computers and Electronics in Agriculture,95, 1-10.

doi:10.1016/j.compag.2013.03.006

Yang, L., Xiantao, H., Tao, C., Dongxing, Z., Song, S., Rui, Z., Mantao, W. (2015). Development

of mechatronic driving system for seed meters equipped on conventional precision corn planter.

International Journal of Agricultural and Biological Engineering, 8(4).

Yeon, J. & Shaw, L. N., 2004. A seed transport and delivery mechanism for revolving spade

planter. Ottawa, Ontario, Canada, American Society of Agricultural Engineers.

Zhao, S., & Chen, Y. (2015). Seed Distribution in Soil and its Effects on Early Plant

Growth. Applied Engineering in Agriculture, 415-423. doi:10.13031/aea.31.10846

Appendix A - Downforce Test Stand

Overview of the design of the test stand's mechanics

The overall design of the downforce test stand uses a scissor-lift mechanism to maintain the

upper row-unit engaging plate in a horizontal position. The mechanism uses two "scissor" arms

on either side that are attached to the upper and lower plates through shafts and pillow block

bearings on one side whereas the opposite sides are allowed to move fore and aft in cam grooves

via cam followers. The length of the cam follower grooves constrains the system to a minimum

and maximum height to prevent damage to the airbag. The airbag is mounted on a 1:1 ratio

trunnion to transfer vertical load from the row unit to a horizontal tension that the stand's load

cell measures. The airbag was chosen so that the test stand could handle a maximum load of

1000lbs with air supplied at 80PSI. An overview of the entire stand mechanism can be seen in

Figure A-1
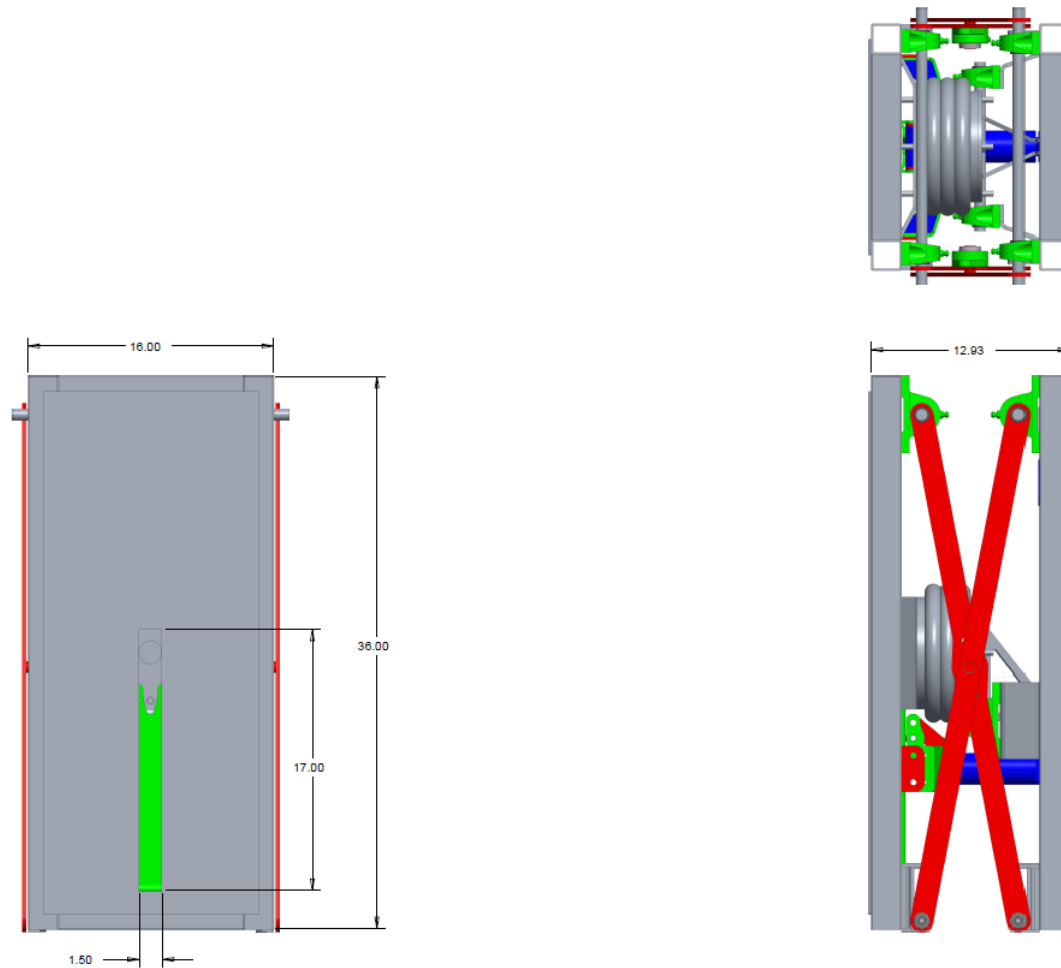
Figure A-1 Test stand drawing showing top, side, and end views with overall dimensions

The disc load mechanism simulates soil resistance through the use of a pneumatic cylinder. The

entire mechanism is fixed to the upper platform of the test stand so that any load applied by the

row unit discs is measured through the stand load cell. A linkage and roller mechanism transfers

force from the pneumatic cylinder to the disc channel. This linkage is designed in a 2:1 ratio to

amplify the force applied by the pneumatic cylinder. The system is designed to carry a mximum

disc load of 300lbs at 120 PSI of supplied air pressure. This allows for a small-bored pneumatic

cylinder to be used to reduce test stand cost. By amplifying the force produced by the pneumatic

cylinder a lower air pressure can also be used. An overview of the disc loading system can be

viewed in Figures A-2 and A-3.
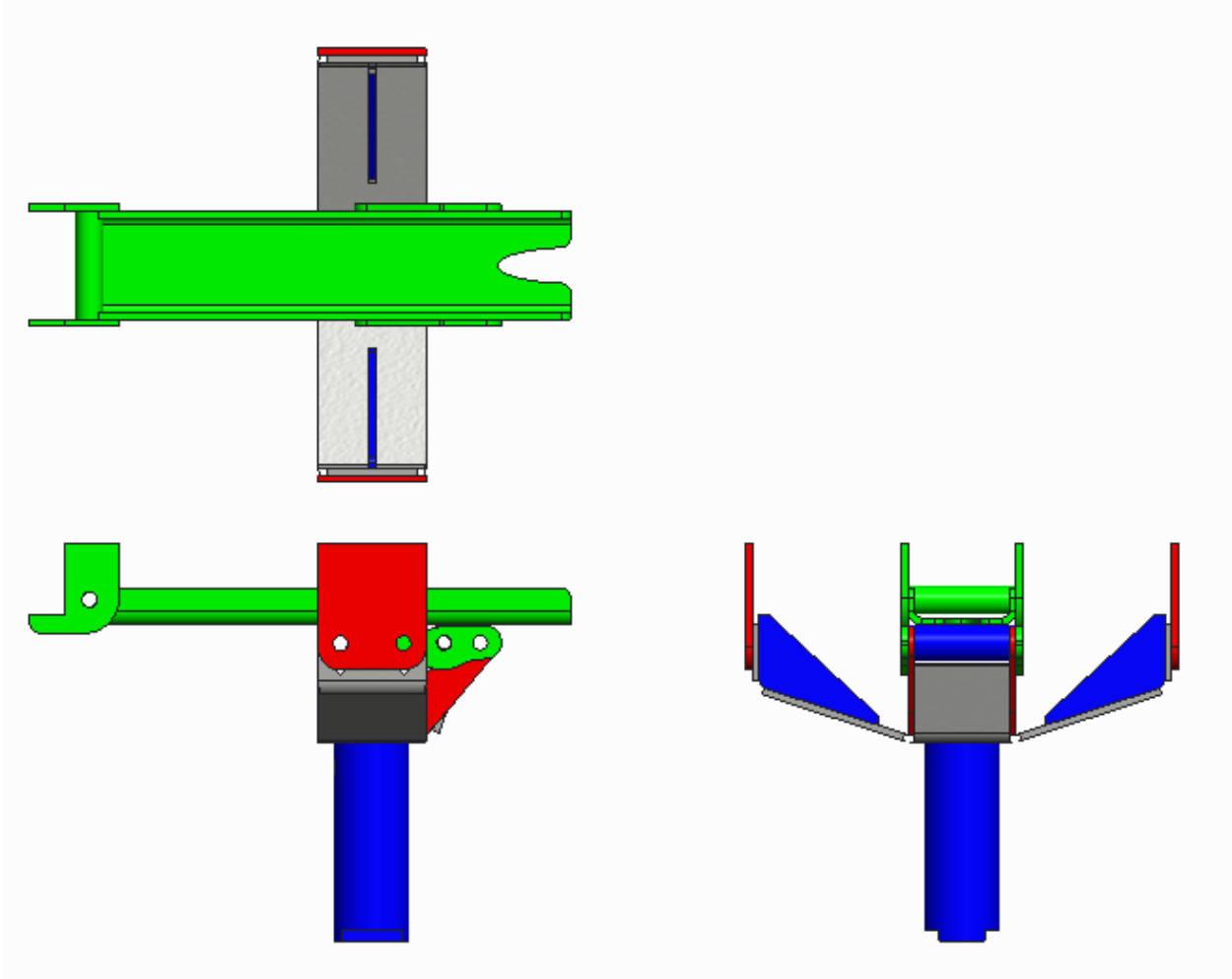
Figure A-2 Disc load mechnism drawing; top, side and front views shown
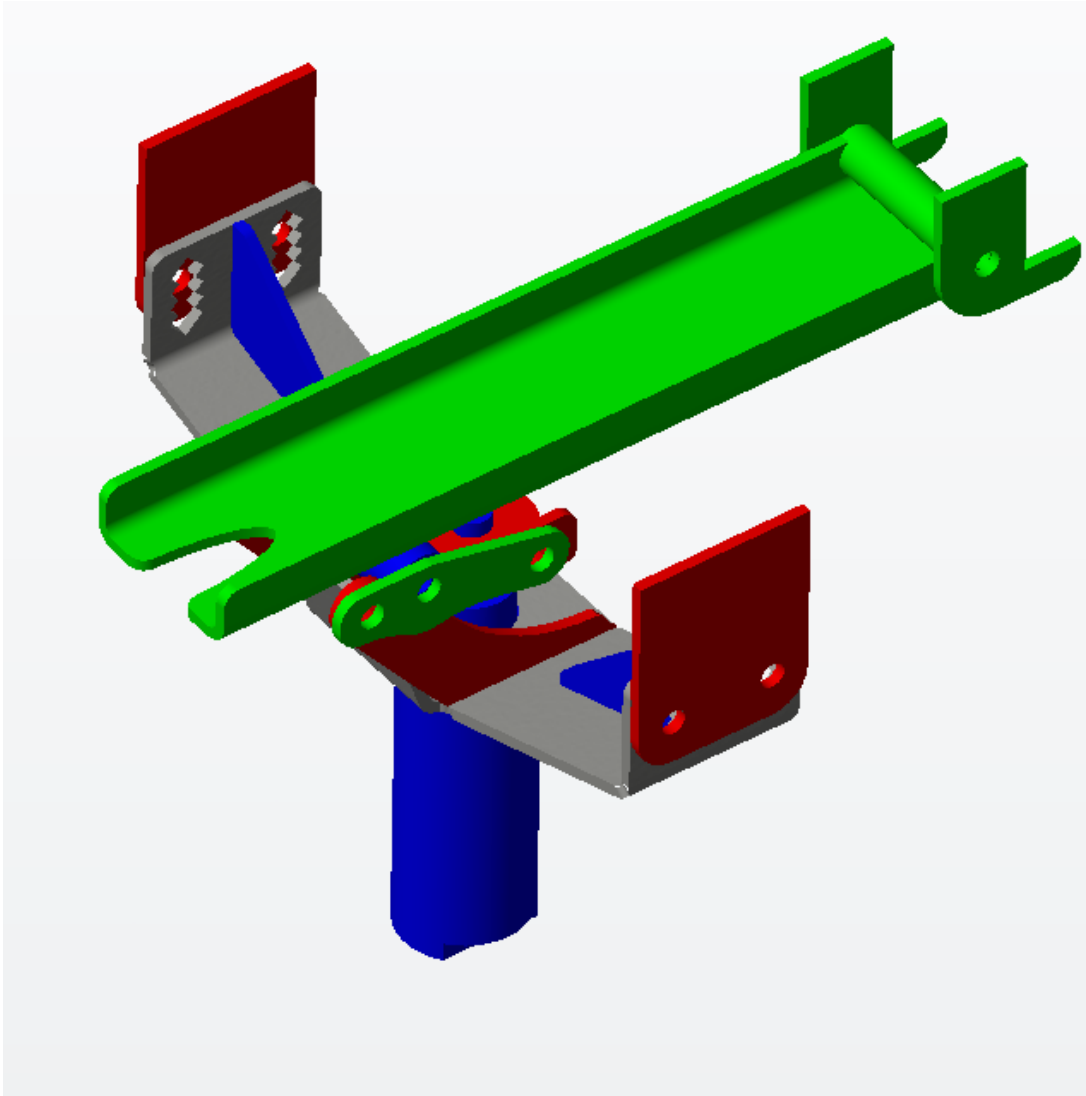
Figure A-3 Disc load mechanism isometric view

Both stand load mechanisms are mounted to the upper stand plate that engages the row unit. By

mounting the disc load mechanism to the upper plate, the total load exerted by the row unit can

be measured through the test stand load cell mounted to the airbag trunnion. This system can be

overviewed in Figure A-4.
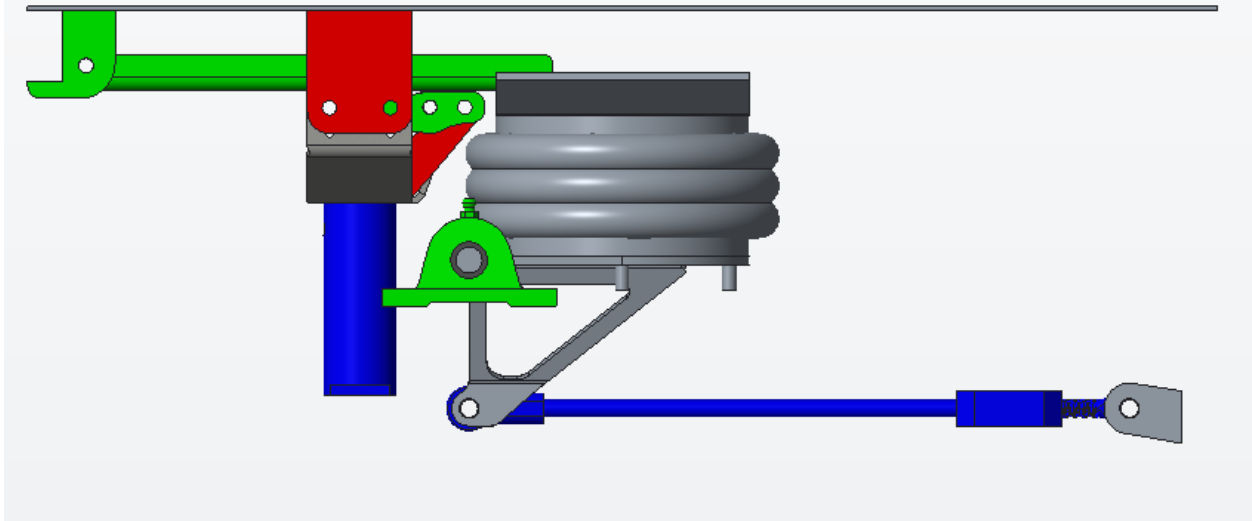
Figure A-4 Disc load and airbag load mechanisms shown with reference to stand top plate

Pneumatic system sizing and component selection

After selecting the pneumatic loading components for the test stand, the required flow rates for

each component under full load were calculated. To move the airbag, at a full load of 1000lbs

0.5" in one second, a compressed air flow rate of 0.22cfm is required at 80psi. To load the disc

cylinder to 350lbs an air flow of 0.15cfm was needed at 120psi. With both pneumatic load

components combined, the compressed air supply would need to supply approximately 0.5cfm of

airflow at 120psi. The airflow requirement was rounded to 0.5cfm to account for the effects of

flow loss through the pneumatic hoses connecting the components. The calculations for the disc

cylinder and airbag can be seen in Figure A-5.
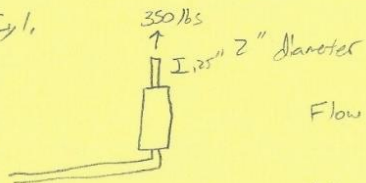
Figure A-5 Test stand airbag and disc load cylinder compressed airflow requirements

After determining the required air pressure and flow rates for each component on the test stand, the pneumatic valves that would increase and decrease the load applied by each component were sized. Using the valve's Cv value and a pressure difference of 1psi across the valve an air flow was calculated. A pressure differential of 1psi was used to represent the worst case scenario where a load component's pressure is closest to the compressed air supply pressure. It was found that a 3/8" pneumatic solenoid valve would be sufficient for operation of the disc load cylinder and a ½" pneumatic solenoid valve would be sufficient for the airbag system. Also calculated was the pressure drop that would occur during maximum air flow requirements through the 3/8" air supply line. Because the utilized shop air supply operates at 130psi and the maximum required pressure for the test stand was 120psi, the 3.3psi pressure drop is acceptable. The calculations for valve sizing can be seen in Figure A-6.

3/8" valve   DVP-2DC3F-24D

$C_V = 0.315$

$$Q = 13.63 \times C_v \times P_1 \sqrt{\frac{1}{T(°R) \times S_g}}$$

$$Q(scFm) = 13.63(0.315)(125+14.7)\sqrt{\frac{1}{(459.7+75)(1)}} = 25.94 \, scFm$$

(Max flow at base pressure charge = 25.94)

$$Q(scFm) = 13.63(0.315)(125-124)\sqrt{\frac{1}{534.7}} = 0.19 \, scFm$$

Flow of 0.19 scFm @ 1psi pressure difference

½" valve   DVP-2BC4A-24D $C_V = 2.45$

$$Q = 13.63(2.45)(80-79)\sqrt{\frac{1}{534.7}} = 1.44 \, scFm$$

large Valve @ 1 psi pressure difference   Q = 1.44 scFm

Shop airflow, 130psi supply, 3/8" airhose

$$Q = 13.63(1)(\Delta p)\sqrt{\frac{1}{534.7}}$$

$$\Delta p = 3.39 \, psi$$

**Figure A-6 Valve flow rate calculations at maximum component loading**

83

Electronic control and data acquisition system

To control the pneumatic solenoid valves, the National Instruments CRio chassis output

command signals via a NI 9476 module. The module was used to switch a 15VDC signal on and

off that, in turn, controlled 70G-ODC15 relays. The relays switched 24VDC to directly control

the solenoid valves. The relays were mounted in a 70GRCK4R chassis. An overview of the

solenoid control system can be seen in Figure A-7.
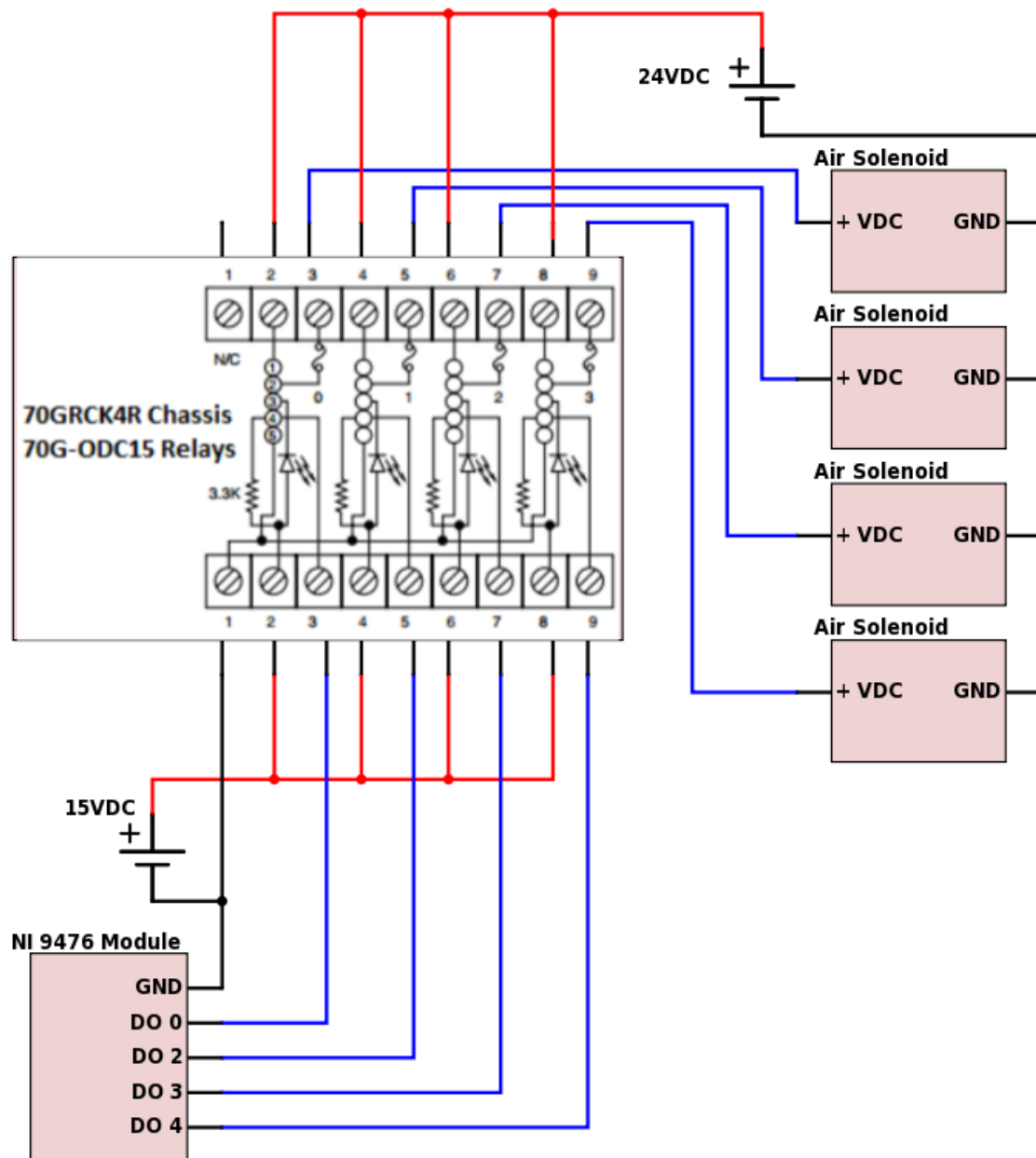
Figure A-7 Pneumatic solenoid control schematic showing connections from NI module to solenoid valves

To gather sensor data, several NI C-Series modules and sensors were used. The sensors gathered the test stand's loading and monitored the hydraulic system's pressures. To gather overall test stand load, a 1000 lb loadcell was placed between the airbag trunnion and the stand's frame. The total load measured by this sensor is the sum of the row unit's disc load, gauge wheel load, and

closing wheel load. To distinguish between the loads applied by the opening discs vs. the gauge wheels, the planter row unit's gauge wheel load pin was measured to gather only the gauge wheel load. This load was used, along with the force applied by the closing wheels in a particular setting, to determine the opening disc load that was being applied to the stand. Because the planter's ECU used the gauge wheel load pin for automatic downforce system control, the sensor was read by a Ni 9203 C-Series module and then output to the ECU via a NI 9265 C-Series module. The gauge wheel load pin data was repeated at 100Hz, the same rate that the planter ECU sampled the sensor, to ensure the ECU control is not affected by the data acquisition system.   A schematic of the sensor connections and load pin output can be viewed in Figure A-8.
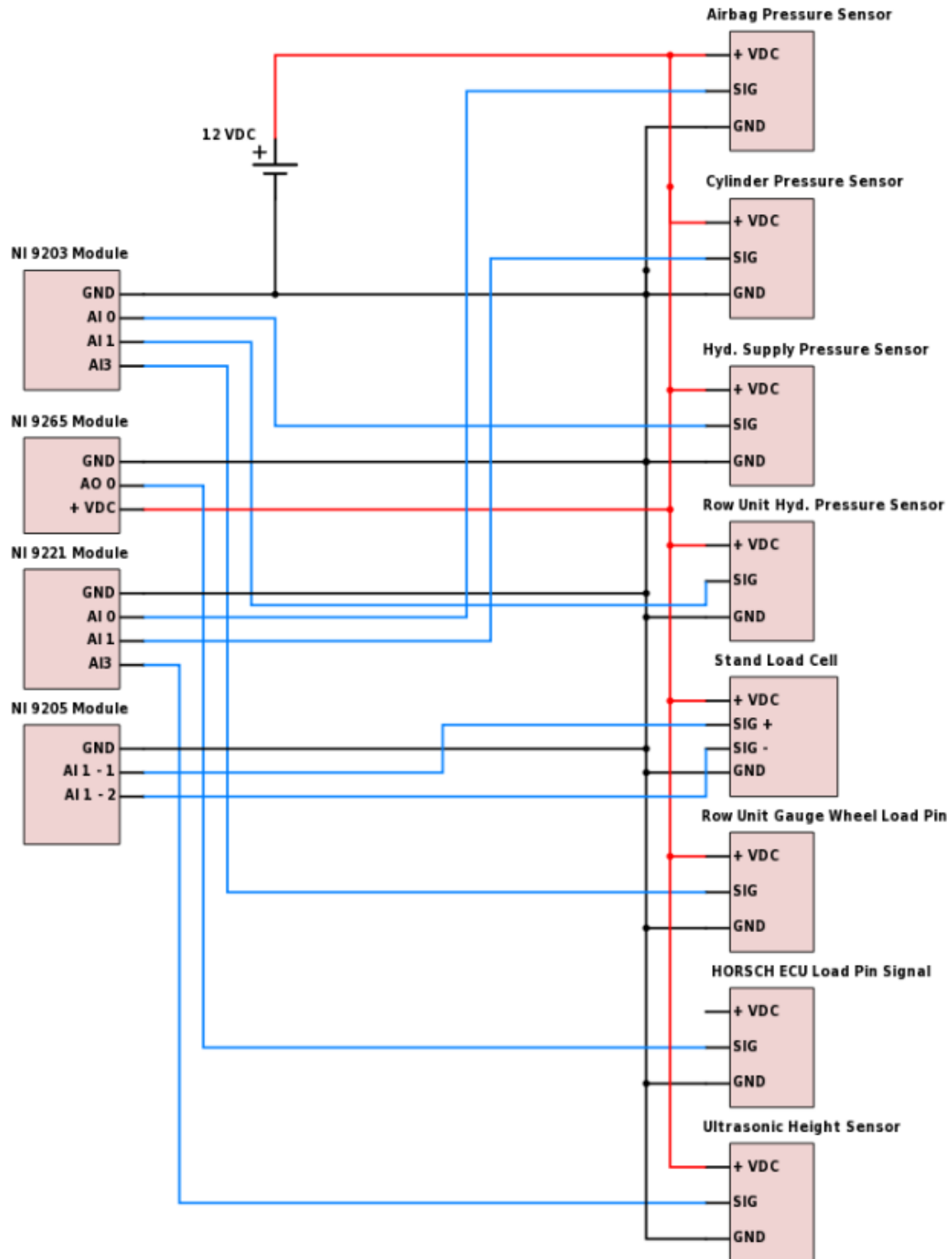
Figure A-8 Electrical connections between NI modules and various sensors located on the test stand and row unit